NATIONAL UNIVERSITY OF SCIENCE AND TECHNOLOGY
BUCHAREST POLYTECHNIC

DOCTORAL SCHOOL OF ELECTRICAL ENGINEERING

EXTENDED ABSTRACT
Ph. D. THESIS

Contributions to the application of electric circuit theory in the design and optimization of an intelligent battery management system for electric vehicles

Ph. D. Supervisor:
Prof. Dr. Eng. Mihai IORDACHE

Ph. D. Student:
Eng. Mihai Rotaru

BUCHAREST
2026

TABLE OF CONTENTS

Chapter 1. Introduction 3
1.1. Presentation of the doctoral thesis 3
1.2. Purpose of the doctoral thesis 3
1.3. Content of the doctoral thesis 4
Chapter 2. Dynamic Asynchronous Motor Analysis 5
2.1. Introduction: Interaction between the traction consumer and the storage system 5
2.2. Analysis taking into account the magnetisation characteristic and the variation of rotational resistance with slip 5
2.3. Variable reluctance engine analysis 7
2.4. Observations and conclusions 7
Chapter 3. Generating parameters of dual-port circuits and analog filters 9
3.1. Introduction: The Need for Modeling Filter Stages 9
3.2. Generation of parameters of analogue quadripoles and filters in harmonic mode 9
3.3. Example 11
3.4. Generation of transfer functions by the method of half-state equations 11
3.5. Observations and conclusions 12
Chapter 4. Impedance Adaptation in Signal Transmission Lines 13
4.1. Introduction: Optimizing Power Transfer and High-Frequency Communication 13
4.2. Impedance adaptation procedures 13
4.3. Adaptation of tasks; Smith diagram; L, T and Pi networks 14
4.4. Conclusions 15
Chapter 5. Battery Management System (BMS) in the Electric Vehicle Ecosystem 17
5.1. Necessity, vital functions and thermal management 17
5.2. Estimation of SoC and SoH; Cell balancing techniques 18
5.3. The impact of BMS on lifespan: case study (Renault Zoe vs. Nissan Leaf) 20
5.4. Conclusions 22
Chapter 6. Integration of electric vehicles through V2X and V2G technologies 23
6.1. Context, charging connector and two-way communication standards 23
6.2. V2G validations, integration with photovoltaic systems and technical-economic analysis 23
6.3. Conclusions 25
Chapter 7. Design, practical realization and simulation of a BMS system with V2X functions 26
7.1. Introduction and equipment used 26
7.2. System architecture and V2L modeling/simulation in Matlab/Simulink 26
7.3. Experimental results and performance analysis 28
7.4. Conclusions 29
Chapter 8. General conclusions, original contributions and perspectives 33
8.1. General conclusions 33
8.2. Original contributions 33
8.3. List of published works 35
8.4. Prospects for further development 36
Selective bibliography 37

Chapter 1. Introduction

Accelerated transformations in electric mobility and the expansion of the use of renewables are changing the way electricity is produced, stored and used. In this context, the electric vehicle is no longer seen exclusively as an energy receiver, but also as an active storage element, capable of participating in bidirectional power exchanges. Through Vehicle-to-Grid (V2G), Vehicle-to-Home (V2H) and Vehicle-to-Load (V2L) technologies, the energy stored in the battery can be redirected to the grid or to various local consumers, giving the vehicle an extended functional role within modern energy systems [1]–[3].

The reliable application of these concepts requires an in-depth analysis of the subsystems that make up the energy architecture of an electric vehicle. The operation of electronic converters introduces non-sinusoidal regimes that influence both the behavior of electric traction machines and the overall performance of the assembly. In parallel, it becomes necessary to carefully design interface filters, correctly adapt impedances on communication lines and implement a high-performance battery management system, capable of ensuring the supervision, protection and efficient operation of cells [4], [5].

The proposed research aims to coherently integrate the notions of electric circuit theory in the analysis and development of solutions applicable to the electric vehicle ecosystem, with a focus on optimizing energy flows and capitalizing on the bidirectional capabilities of batteries.

1.1. Presentation of the doctoral thesis

The thesis aims to investigate, model and optimize the energy processes specific to electric vehicles, focusing on the integration of V2X functions and the role of the intelligent battery management system. The approach starts from the foundations of circuit theory and aims to transfer them to current applications, relevant for charging infrastructure, power conversion and flexible exploitation of stored energy.

The approach includes the modeling of tensile elements and interfacing circuits, as well as the analysis of structures used for filtration, impedance adaptation and energy control. This theoretical basis is then extended to the study of BMS systems, which are essential for the safe and efficient operation of Li-Ion batteries. A central point is the demonstration of the possibility of using batteries in electric vehicles not only for propulsion, but also as bidirectional energy resources, compatible with residential hybrid systems that include photovoltaic generation.

1.2. Purpose of the doctoral thesis

The recent evolution of battery management systems has been driven by the need to limit electrochemical degradation and increase the lifespan of Li-Ion cells [6]–[8]. If the first generations of electric vehicles were affected by sharp decreases in range, current solutions are based on advanced monitoring and estimation algorithms, capable of tracking the individual state of the cells and applying effective balancing strategies. Thus, the BMS has become a critical subsystem for maintaining the safety, performance and reliability of the entire battery pack [9], [10].

The implementation of V2X technologies involves overcoming technical difficulties that go beyond the mere existence of a communication standard. Although frameworks such as ISO 15118 provide support for the exchange of information, the practical realization of the physical interface involves robust solutions for impedance adaptation, electromagnetic compatibility and the design of converters capable of operating under deforming conditions, without affecting the stability of the network or the operation of the traction system. The aim of the thesis is to develop an integrated perspective on these issues, from the point of view of circuit theory and engineering applicability [11], [12].

1.3. Content of the doctoral thesis

The paper is organized into eight chapters, designed to follow a logical path, from the theoretical bases of modeling electrical circuits and systems to the experimental validation of a BMS solution with V2X functions.

The first chapter introduces the general context of the research, presents the relevance of the topic and formulates the main objectives. The second chapter is dedicated to the analysis of the asynchronous motor in dynamic mode and highlights the influence of nonlinearities and harmonics on the performance of the traction system, through simulation tools and methods for analyzing the behavior of the electric car in complex operating conditions [13]–[16].

In the third chapter, methods are developed for generating the characteristic parameters of biport circuits and analog filters, with emphasis on obtaining symbolic and numerical-symbolic expressions useful for the exact modeling of interface networks. The fourth chapter deals with impedance adaptation in transmission lines, with a focus on the use of the Smith diagram in the design of adaptation structures specific to high-frequency circuits [17]–[20].

Chapter five looks at the architecture and functions of the battery management system, focusing on the estimation of internal parameters and cell balancing techniques, including a comparative study on the degradation of batteries used in commercial electric vehicles. The sixth chapter extends the analysis to the integration of electric vehicles in V2X applications and discusses both the aspects of two-way communication and the technical-economic implications of using the vehicle battery as a flexible energy resource [21], [22].

The seventh chapter brings together the applicative contributions, by presenting an experimental BMS assembly with V2L function and by modeling it in a simulation environment, aiming at validating the power transfer and correlating the experimental results with the theoretical ones. The last chapter summarizes the general conclusions, the original contributions and the directions for further research.

Chapter 2. Dynamic Asynchronous Motor Analysis

2.1. Introduction: Interaction between the traction consumer and the storage system

The performance of an electric vehicle and its ability to integrate into V2X or V2G applications depend directly on the correlation between the traction and energy storage subsystems. The design of an efficient BMS cannot be separated from the analysis of the operating regime of the electric car, and the development of filtration solutions and adaptation structures for bidirectional communication requires accurate knowledge of the sources of disturbances generated in the power assembly.

The asynchronous motor, frequently used in modern electric propulsion systems, has a complex and pronounced nonlinear dynamic behavior. The magnetic saturation of the ferromagnetic circuit, together with the variation of rotoric parameters (the effects associated with slippage and current distribution in conductors), influences the shape of currents and voltages. When these nonlinearities overlap over the switching processes of the static converters, the result is a pronounced deforming regime in the vehicle's internal network [17], [23].

The harmonics generated not only affect the motor, but also propagate to the DC source, increasing the energy and thermal stress on the battery. Additional losses occur, conversion efficiency is reduced, and system operation becomes more difficult to control. Therefore, before developing a BMS architecture for bidirectional transfer, it is necessary to rigorously evaluate the primary sources of harmonic deformation, by analyzing the asynchronous motor in dynamic mode and by mathematically substantiating its behavior with the help of specialized simulation programs [14]–[16], [24], [25].

2.2. Analysis taking into account the magnetisation characteristic and the variation of rotational resistance with slip

The analysis of electromagnetic systems periodically excited by complex signals is of both theoretical and applicative interest. In electricity networks, deviation from the ideal sinusoidal regime is associated with a deforming regime produced by nonlinear elements or constructive imperfections of the sources and consumers. Important causes include the non-sinusoidal distribution of induction in the interfier, saturation of ferromagnetic cores, the presence of power electronics, and the operation of highly nonlinear loads [23].

For the investigation of non-sinusoidal periodic regimes, numerous methods have been developed, divided into two categories: methods formulated in the time domain (variants of the shooting method – SH) and methods developed in the frequency domain (forms of the harmonic balance method – HBM). The choice of method depends on the structure of the circuit, the degree of nonlinearity and the precision sought in highlighting harmonics [24], [26]–[27].

The model used starts from the equivalent scheme in Π of the induction motor, in which the magnetization inductance is introduced in the form of a nonlinear coil controlled in the

current, and the rotating resistance is considered variable in time, depending on the slippage. This choice allows the realistic representation of the influence of magnetic saturation and the change of rotoric parameters on the response of the system [14], [15], [24].

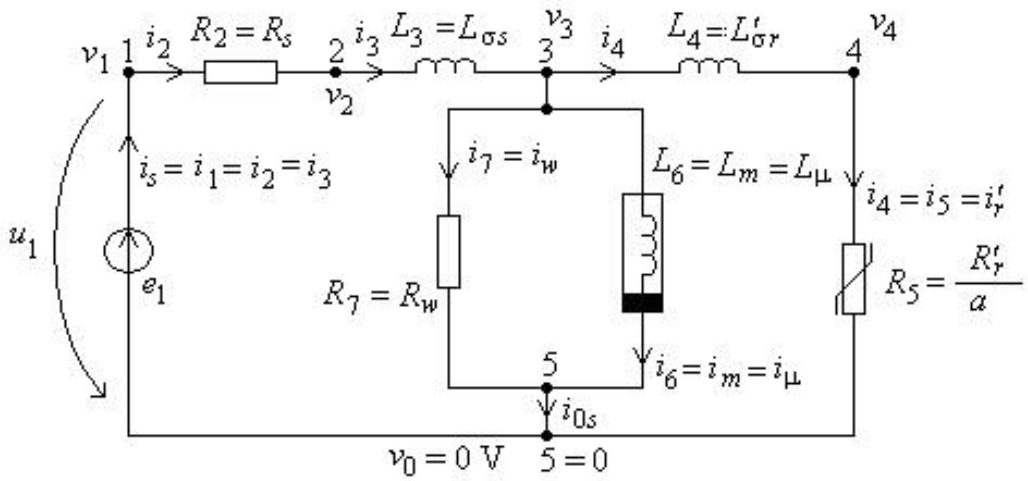


Figure 2.1. The equivalent diagram in Π of the induction motor.

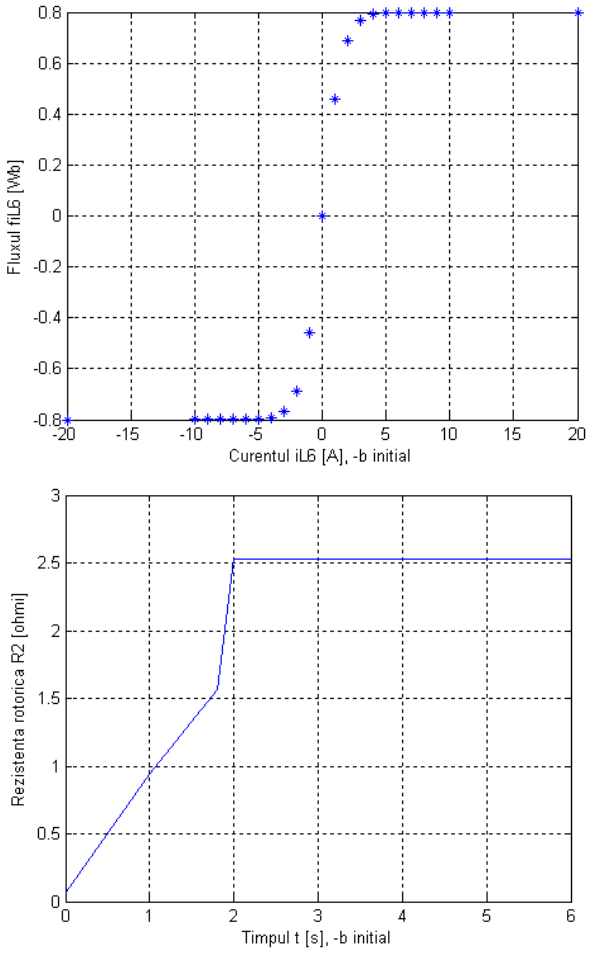


Figure 2.2. a) Characteristic Lm(iLm) = L6(iL6); b) Characteristic R2(t).

The symbolic-normal equations of state for the induction motor are integrated with the integration routines in the MATLAB environment [19]. The modified nodal equations, obtained by the Euler algorithm of implicit integration, are solved at each step of time, the

magnetization characteristic being approximated by line segments. The netlist input file, required by the ACAP program, describes the circuit topology and the nonlinear characteristics given by the dots [18].

For the simulation of the current-controlled nonlinear coil in SPICE, an equivalent diagram based on controlled sources is used, in which the voltage-controlled nonlinear resistor has the same characteristic as that of the current-dependent flow. The results obtained with the ACAP and SPICE programs were compared by time domain analysis and Fourier analysis of current and voltage waveforms.

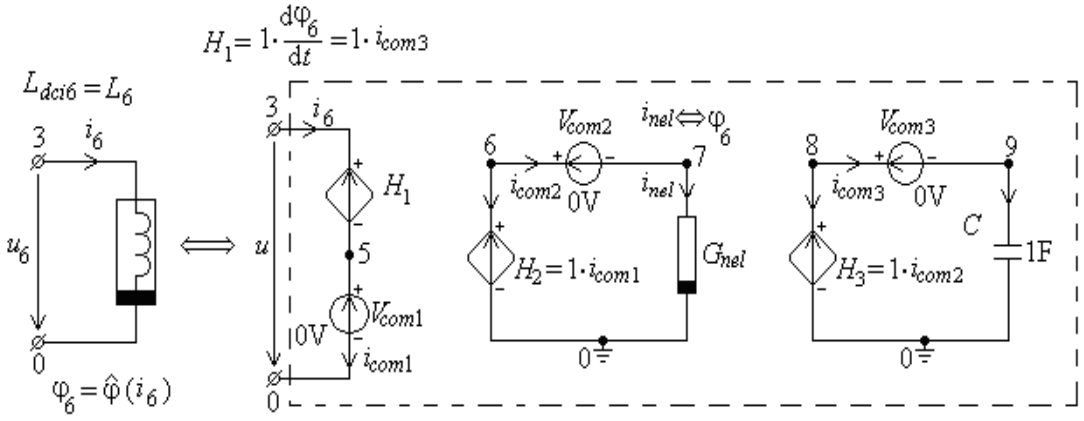


Figure 2.3. Simulation in Spice of current-controlled nonlinear coils.

2.3. Variable reluctance engine analysis

The variable reluctance motor is a single-phase AC motor, the operation of which is based on the change in inductivity. From the perspective of design and operation, it is important to know the variation of currents in transient regime. Based on the numerical values of the parameters of the equivalent circuit, the variations in time of the currents in the transient regime occurred when connecting the motor to the power supply network were determined, with zero initial conditions.

By running the ACAP program via MATLAB, with the corresponding input file, the time variations and Fourier analysis of the voltages and currents in the circuit were obtained. The results were validated by simulation in SPICE, finding a very good concordance between the two programs [28], [19].

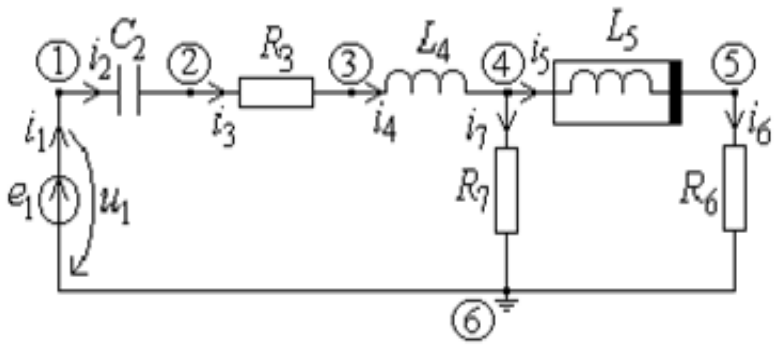


Figure 2.4. The equivalent circuit of the variable reluctance motor.

2.4. Observations and conclusions

In this chapter, the influence of magnetic saturation on the performance of the induction motor was investigated, starting from the equivalent scheme in Π, in which the magnetization inductance was modeled as a nonlinear coil driven in current, and the rotor resistance was considered variable in time. The simulations were carried out with the ACAP, CSAP and SPICE programs, all based on the formulation of modified nodal equations and capable of providing Fourier analysis of waveforms.

The results highlight that the presence of higher-order harmonics leads to increased copper and core losses and decreased yield and power factor, while the electromagnetic torque developed increases significantly. The originality lies in the fact that the ACAP, SYSEG and CSAP programs can analyze analog circuits in a completely symbolic, numerical-symbolic or numerical way, allowing the consideration of parameters of the equivalent circuit as symbols and the analysis of the performance of the motor in different working modes. For the integration of linear and nonlinear differential equations, MATLAB routines were used, very effective for this type of equations.

Chapter 3. Generating parameters of dual-port circuits and analog filters

3.1. Introduction: The Need for Modeling Filter Stages

The analysis of the deformed regimes associated with static power conversion highlights the need for rigorously designed filter stages. The switching of inverters, together with the nonlinearities of electric cars, degrades the power quality and can affect the electromagnetic compatibility of the assembly. In the absence of adequate filtering structures, the energy transferred bidirectionally between the vehicle and the grid may exceed the permissible limits for the total harmonic distortion and the level of conducted disturbances.

The sizing of filters and interfacing networks requires a faithful modeling of the two-port circuits. The classical descriptive parameters (Z, Y, T, H) remain useful in theoretical analysis, but their direct application to high frequencies is experimentally difficult. Therefore, in the design of high-frequency circuits, it becomes essential to use scattering parameters (S) and conversion procedures between the different representations. The chapter develops the theoretical and numerical framework necessary for the automatic generation of transfer functions and parameter matrices for passive linear quadripolar networks.

3.2. Generation of parameters of analogue quadripoles and filters in harmonic mode

3.2.1. Theoretical issues

The behavior of two-gate linear networks in harmonic mode can be described by several parameter families. At low and medium frequencies, the Z, Y, H, T or F matrices are used, which allow the compact formulation of the relationships between the voltages and currents of the ports [31], [26], [32]–[34]. As the frequency increases, the experimental conditions for determining these parameters become more difficult to achieve.

In the field of microwaves and high-frequency communications, the characterization of networks is based on scattering parameters, since at such frequencies the measurable quantities are incident, reflected and transmitted waves. The S-parameters provide a direct description of reflection and transmission phenomena, without imposing difficult test regimes (idling or ideal short circuit), being indispensable in the analysis of RF circuits, high-frequency integrated components and galvanic contactless energy transfer structures [34]–[38].

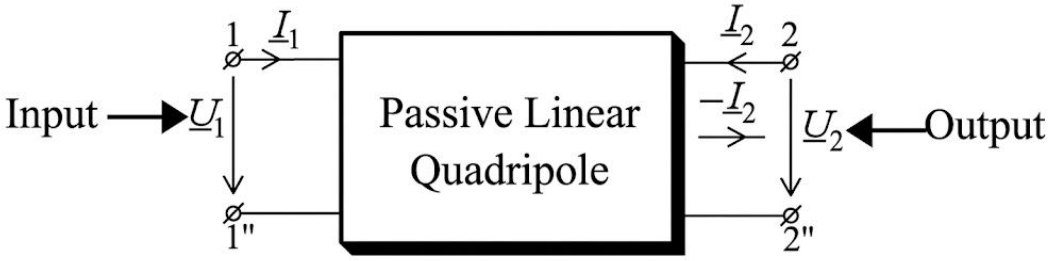


Figure 3.1. Diagram of the passive linear biport circuit.

For a passive linear bicarrier, the equations expressed by the fundamental (transfer) parameters in harmonic regime link the quantities of one gate to those of the other: U1 = A· U2 + B· I2 and I1 = C·U2 + D·I2. Starting from these relations, the equations in transfer impedances (Z), transfer admittances (Y), hybrid parameters (H) and F parameters (inverses of hybrids) are obtained, each set being adequate to the description of certain devices [16], [33], [17].

A passive linear quadripole is reciprocal if the determinant of the fundamental matrix satisfies AD − BC = 1, a condition equivalent to specific relations between the parameters Z and Y. The reciprocal quadripole is symmetrical if A = D, i.e. if the two gates can interchange without changing the equations. For a passive linear quadripole, the characteristic impedances and image impedances are also defined, expressed according to the fundamental parameters [31], [26], [29], [30].

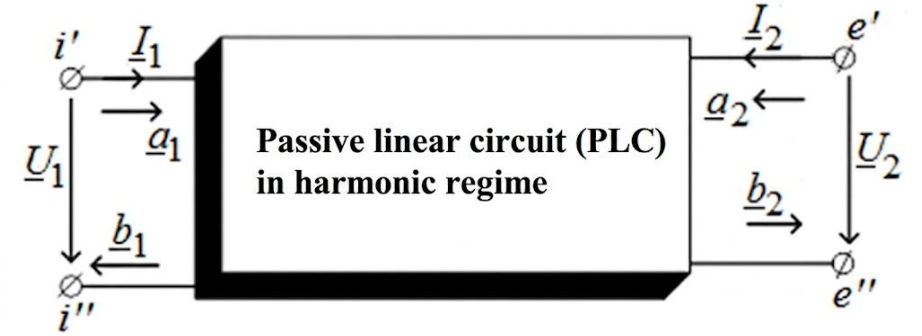


Figure 3.2. Circuit used to define parameters S.

3.2.2. Automatic generation of transfer functions and conversion between parameters

The conversion between S-parameters and classical representations of quadripoles is of major practical importance, as it allows the transition from experimentally achievable measurements (with the network analyzer) to quantities useful in design. A measured dataset can be transformed into Z, Y or T parameters, facilitating the sizing of filters, the assessment of adaptation and the estimation of the energy performance of the structure [34]–[39], [16].

The calculation procedures start from the defining relationships of the parameters Z, Y, T, H and F and lead to the generation of the associated transfer functions. The implementation is carried out by both modified nodal equations and equations of state, so that the methodology can be flexibly applied to different circuit configurations. In order to generate the parameters S according to the elements of the matrix of the fundamental parameters T, the MAPLE environment proceeds by expressing the variables U1, U2, I1, I2 according to the waves a1, a2, b1, b2 and the reference impedance Z0, solving the system and identifying the coefficients S11, S12, S21, S22.

Implementations developed in MAPLE and MATLAB automate traditionally laborious and error-prone computational steps. Through this automation it becomes possible to quickly compare theoretical results with numerical and experimental ones, as well as to explore the influence of parameters on the overall behavior of the circuit. The method is used for

quadripolar circuits, analog filters, and magnetically coupled coil structures, of interest in wireless power transfer and electric vehicle interfacing stages.

3.3. Example

The proposed procedures were validated by representative examples. For a given quadripole, the fundamental (transfer) parameters are first generated, which involve the simplest transfer functions, and based on them the other parameters (Z, Y, H, F, S) are calculated using the theoretical relations. The required transfer functions are obtained by modified nodal equations, generated with the ACAP, CSAP and TFSYG programs, or by equations of state provided by the SYSEG program [35], [29], [30], [14], [15].

Examples also include magnetically coupled resonator structures relevant to wireless power transfer. Based on the characteristic matrices Z, Y, T, H and S, it becomes possible to precisely delineate the passage and attenuation bands, making it easier to identify the type of filter and its functional properties.

3.4. Generation of transfer functions by the method of half-state equations

For circuits with excess elements (e.g. magnetically coupled resonators in series-to-series connection), transfer functions are generated using half-state equations. The SSEMG (Semi-State Equation Matrix Generation) program, called via MATLAB, allows obtaining the array of H(s) transfer functions for single-input and single-output (SISO) or multiple-input-output (MIMO) systems.

Considering as output quantities the currents through the coils and the voltages on the capacitors, and as input quantities the independent sources of voltage and current, the matrix H(s) with its poles and zeros is generated, after which, through the inverse Laplace transform, the variations in time of the half-state variables and of the instantaneous power supplied to the load are obtained.

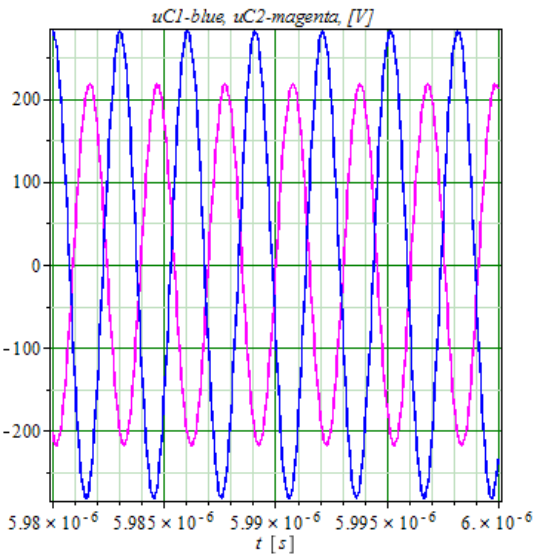


Figure 3.3. Variations in time of the voltages uC1 and uC2 (results obtained by the method of half-state equations).

3.5. Observations and conclusions

The chapter presents advanced methods for generating the characteristic parameters of linear quadripolar circuits and approximate nonlinear circuits by linearization on portions, as well as analog filters. The methodology is applicable to circuits that include excess elements and to any multipole or multiport describable by an equivalent scheme consisting of dipole elements and controlled sources.

The CSAP and TFSYG programs integrate symbolic and numerical calculation techniques: automatic formulation of modified nodal equations in symbolic, partially symbolic or numerical form, generation of circuit functions, analysis in DC, AC and in the operational domain, determination of poles and zeros and construction of modified nodal method matrices. An important advantage is the sensitivity analysis, through which critical elements and permissible ranges of variation of the parameters in relation to the required performance can be identified.

Starting from the defining relations of the fundamental parameters A, B, C, D, the paper proposes efficient procedures for generating transfer functions in fully symbolic, partially symbolic or fully numerical form, followed by the automatic generation of parameters Z, Y, T, H, F and S. In addition to ACAP, CSAP, TFSYG and SYSEG programs, the MAPLE, ANSYS and MATLAB environments contribute to the automation of the calculation process and to the processing of the results [35], [29], [30], [24], [36]–[37]. Dedicated routines allow for rigorous cross-validation, by comparing the numerical results with the data in the literature and with the measurements made on the experimental stand.

Chapter 4. Impedance Adaptation in Signal Transmission Lines

4.1. Introduction: Optimizing Power Transfer and High-Frequency Communication

Filtering harmonic distortions ensures the quality of the voltage and current wave, but the efficient transfer of energy and data packets in V2X systems depends on an additional physical condition: impedance adaptation. At high frequencies, the difference in impedance between the source and the load generates reflected waves, which drastically reduce the efficiency of energy transfer and can damage the power electronics.

Bidirectional charging systems use complex communication standards (such as ISO 15118), which often use Power Line Communication (PLC) technology overlaid over lines of force. Any impedance mismatch causes signal attenuation, protocol errors, and active power losses. In order to cancel parasitic reactants and maximize the power delivered, it is necessary to implement adaptation networks, made either with components with concentrated parameters (inductances and capacitances), or with sections of transmission lines. A central analytical and graphical tool at this stage of design is the Smith diagram.

4.2. Impedance adaptation procedures

Impedance matching refers to adjusting the impedance of a source or load to maximize power transfer or minimize reflections. According to the maximum power transfer theorem, the transferred active power is maximum when the load impedance is the complex conjugate of the source impedance, ZL = ZS*, so that the reactive components cancel each other out [43]–[44].

Where ZS represents the characteristic impedance of a transmission line, the minimum reflection is obtained when ZL = ZS. In a DC circuit the condition is reduced to the equality of the resistors; In alternating current, the reactance depends on the frequency, so the adaptation made to a certain frequency is generally no longer valid outside of it. Broadband retrofitting typically requires complex, filter-like networks, unless the impedances are purely resistive, when a transformer can be used.

Maximum Power Transfer: ZL = ZS* Minimum Line Reflection: ZL = ZS

To assess the degree of adaptation, the Return Loss (PR/RL), which expresses the attenuation of the signal reflected to the source, and the Insertion Loss (IL), which characterizes the diminution of the useful signal introduced by the network, are used. In the ideal case of a perfectly adapted task, PR tends to $-\infty$; in practice, values between approximately 35 and 45 dB correspond to a very good adaptation regime, and short circuit or idle operation corresponds to a return loss of 0 dB [40], [45]–[47].

$$RL = 10 \cdot \log10(Pi / pr) = -20 \cdot \log10|\Gamma| \qquad IL = 10 \cdot \log10(Piece/Insert)$$

By using scattering parameters, the performance of an RF circuit can be fully characterized without knowing its internal structure, the circuit being treated as a "black box" described exclusively by the relationships between the incident waves and those reflected at its gates. The

experimental acquisition of the S-coefficients is performed with the network vector analyzer (VNA), by successively adapted termination of the gates at the reference impedance (usually 50 Ω) [46]–[47].

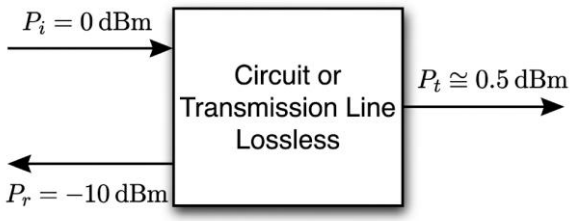


Figure 4.1. Representation of return loss and insertion loss in an ideal transmission line.

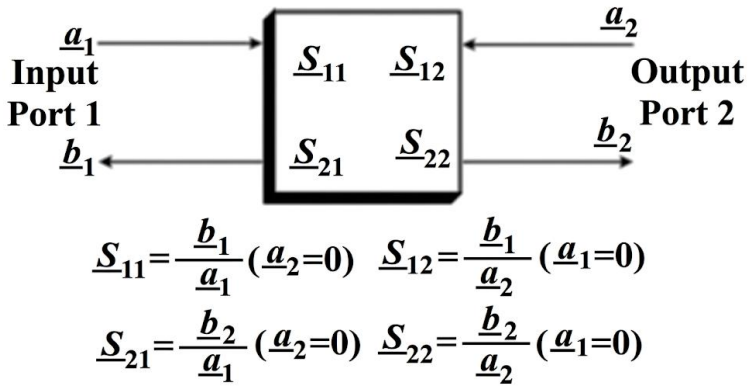


Figure 4.2. Representation of the parameters S for a two-gate microwave circuit.

4.3. Adaptation of tasks; Smith diagram; L, T and Pi networks

The adaptation of a purely resistive load can be achieved using a transmission line with a suitably chosen characteristic impedance, while the adaptation of a complex load is achieved with concentrated passive elements arranged in complementarity (one in series, the other in shunt). Two classical topologies result: the derivation–series configuration and the series–derivation configuration.

The Smith diagram allows intuitive and efficient determination of the circuit elements required for adaptation, both for series and parallel configurations, as well as for combinations thereof. The combined study of the Smith diagram in impedance and admittance representation (imitation diagram) facilitates the tracking of the displacement of the work point and the choice of the optimal configuration, including in the case of adaptation without transmission lines.

For L, T and Pi cross-sectional adaptation networks, the values of the reactive elements are determined analytically. In the case of the Pi network, since there are three elements to be determined and only two equations (equalization of the real and imaginary parts of the impedance equivalent to those of the source impedance), the value of one of the elements is chosen arbitrarily, taking into account the operating frequency, so that the resonant frequencies are close to it. [40], [41]–[42].

Adaptation procedures, including those based on transmission lines, can be easily implemented in computing environments such as MAPLE or MATLAB. Automatic calculation routines of RUST/VSWR parameters, reflection coefficient, power per load and S parameters [42], [45]–[47] are also presented in the literature.

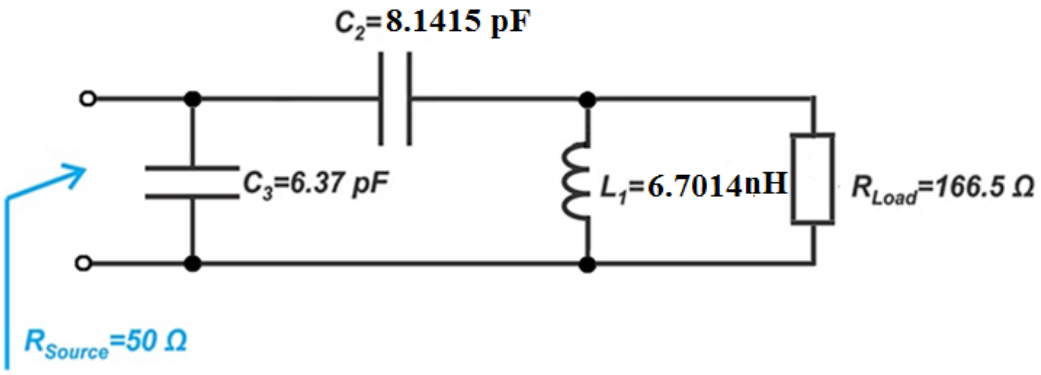


Figure 4.3. Example of a Pi-type adaptation network.

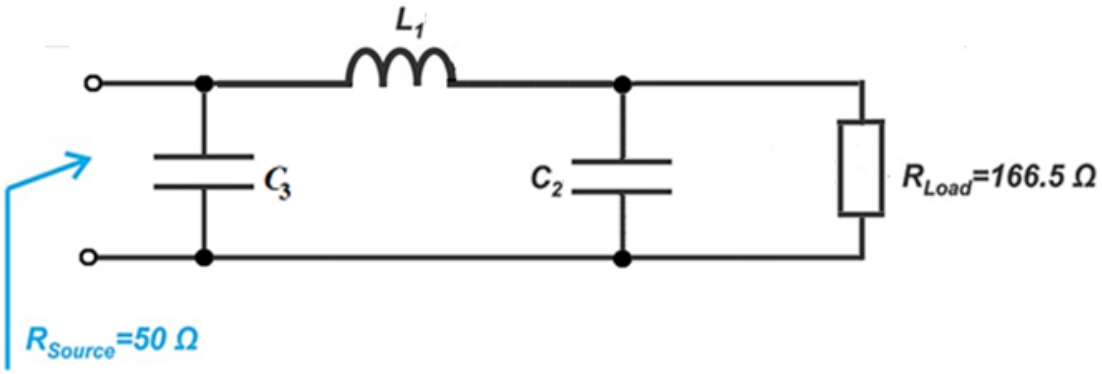


Figure 4.4. Pi network with load resistance connected in parallel with C2 capacity.

4.4. Conclusions

Impedance adaptation is a fundamental design operation, with the objective of either maximizing power transfer or minimizing signal reflections. Its importance is particularly important in analog circuits, wireless power transfer systems, transmission lines, radio frequency interfaces and energy conversion structures operated at high frequencies.

Most adaptation procedures are based on the maximum power transfer theorem. The chapter also includes the presentation of a maximum power point tracking device, used for the efficient extraction of energy from a photovoltaic panel: in relation to the panel, the device follows the principle of maximum power transfer, while at the output the connection is of the impedance bridge type, designed to maximize efficiency by creating a high voltage source type interface with low internal impedance.

An essential role is played by the Smith diagram, widely used for determining circuit elements. In practice, the exact values of coils and capacitors cannot always be implemented identically to the theoretical ones, the real components being available only in standardized series and presenting unidealities (parasitic resistances, tolerances, frequency dependencies).

That is why the design is mostly aimed at understanding how each reactive element shifts the impedance on the Smith diagram, which makes the process considerably more accessible and efficient.

Chapter 5. Battery Management System (BMS) in the Electric Vehicle Ecosystem

5.1. Necessity, vital functions and thermal management

An electric vehicle battery pack consists of a large number of individual cells, connected in series-parallel topologies to ensure the voltages and currents required by the traction. Lithium-ion cells do not have perfectly identical characteristics, resulting in variations in capacity, internal resistance and self-discharge rates. Without strict control, these deviations lead to the overloading of weak cells and the underloading of those with higher capacity.

The Battery Management System (BMS) acts as a central decision-making unit: it monitors operating parameters, coordinates energy exchange with external infrastructure and protects the battery against destructive regimes [4], [5], [7]. The manufacturer's safety reserve limits the state of charge, as the battery is never fully charged or physically discharged; the difference between the technical and operational SoC is an essential protection measure. The BMS architecture integrates sampling circuits, microcontrollers for estimating internal states and communication modules (CAN bus).

Heat generation is inherent in the processes of charging and discharging. The optimum operating temperature of Li-Ion cells is in the range of 15–35 °C [8]; exceeding these limits accelerates degradation or reduces available capacity. Thermal Management (BTMS) prevents thermal packaging by monitoring the temperature of coolant and modules and automatically limiting power to the detection of overheating. Cooling solutions range from air (forced or passive, below 1 kW) to liquid (direct contact with dielectric liquids or indirectly, through water-glycol mixture cooling plates), to which are added emerging solutions such as phase change materials (PCM), heat pipes and thermoelectric cooling [4], [48].

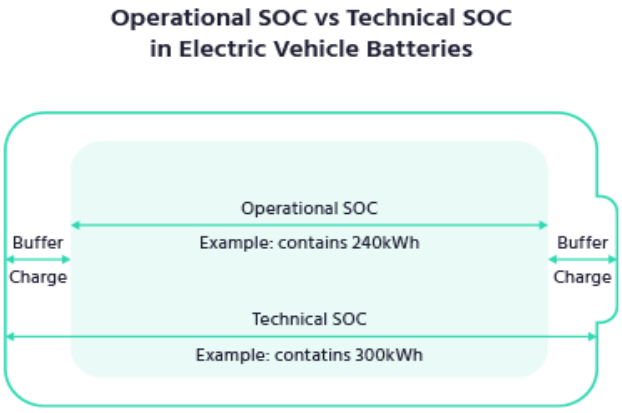


Figure 5.1. The difference between operational SoC and technical SoC.

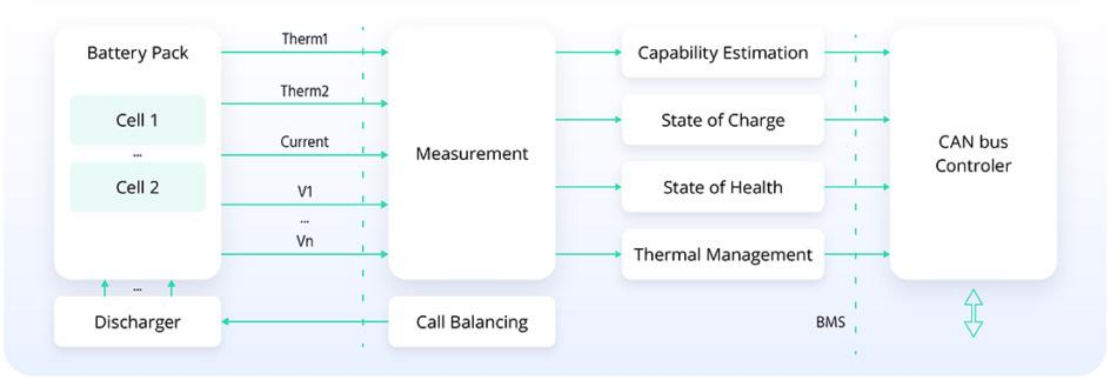


Figure 5.2. Block diagram with the operation of the BMS system.

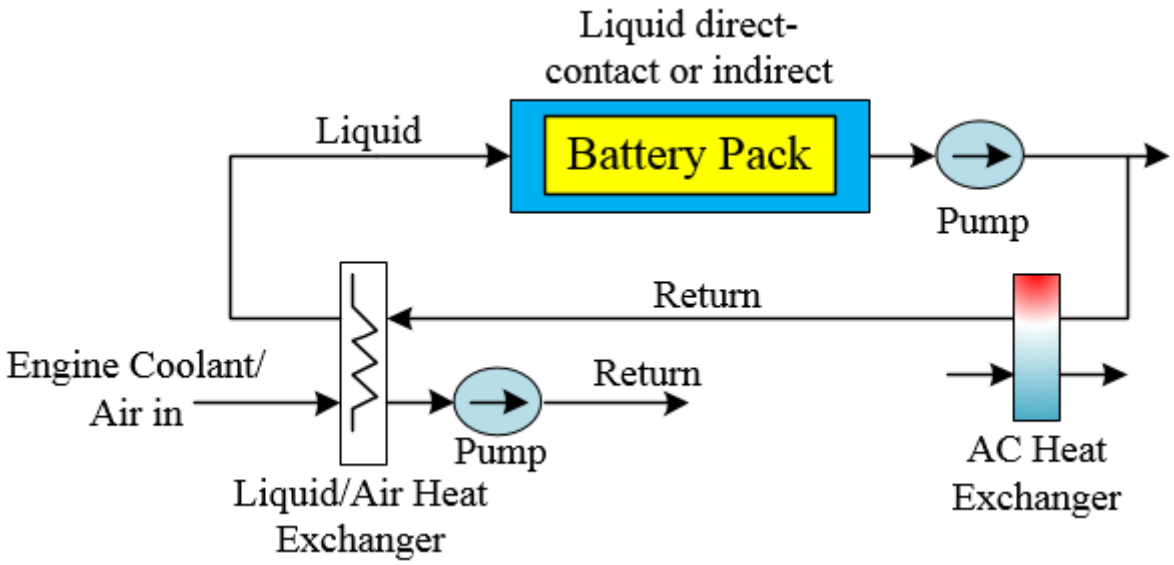


Figure 5.3. Block diagram of thermal management (liquid cooling).

5.2. Estimation of SoC and SoH; Cell balancing techniques

The state of charge (SoC) expresses the ratio of available energy to the maximum usable capacity. Its determination is difficult due to the nonlinear nature of electrochemical processes. The classical method of current integration (Coulomb counting) progressively accumulates errors; to limit drift, modern BMS systems use equivalent circuit models (ECM) correlated with recursive algorithms such as the extended Kalman filter, which continuously corrects the estimate in relation to the open circuit voltage (OCV) [6], [10], [49], [50].

Health status (SoH) is a degradation metric, defined as the ratio of current maximum capacity to nominal capacity. Loss of capacity occurs from parasitic reactions at the electrolyte-electrode interface (SEI) [8]; The SoH drop below 70–80% indicates the end of the useful life in traction mode (EOL), with the battery being able to be relocated to stationary applications.

Balancing maintains an even distribution of charge levels, as a single discharged cell stops the operation of the entire pack. Passive balancing dissipates excess energy on shunt resistors, being simple and cheap, but energy-efficient and heat generators. Active balancing uses DC-

DC converters to transfer the load from heavily charged to deficient cells (cell-bypass, cell-to-cell, or cell-to-pack architectures), recovering power and maximizing usable capacity, at the cost of greater hardware complexity [9].

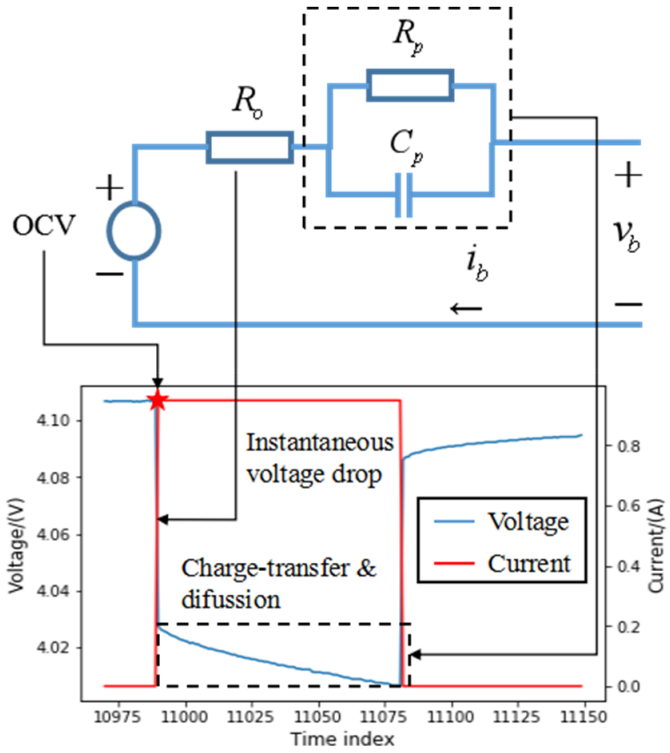


Figure 5.4. RC equivalent circuit model of the battery.

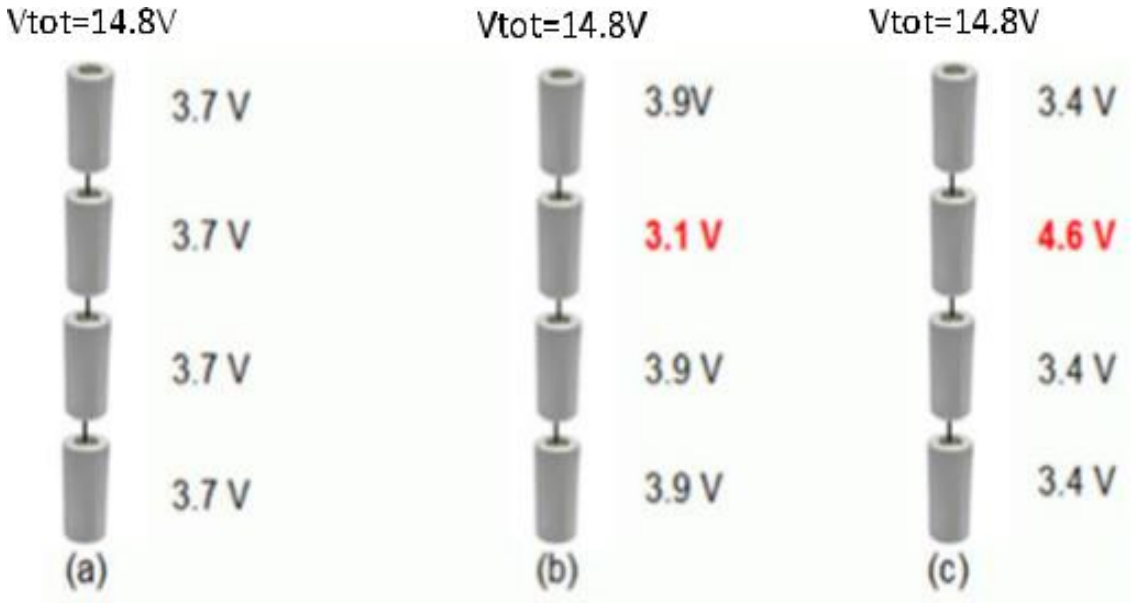


Figure 5.5. Example of variations in cell loading.

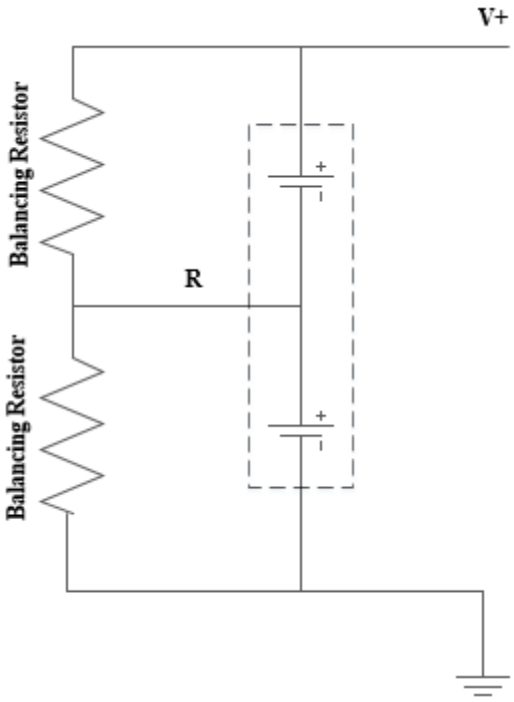


Figure 5.6. Passive balancing circuit.

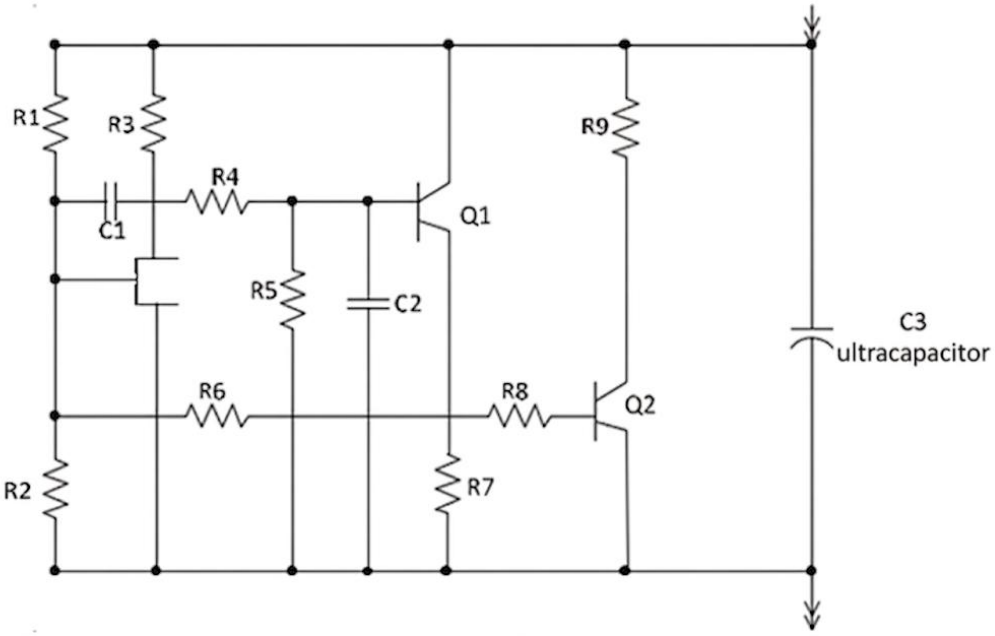


Figure 5.7. The circuit of the active cell balancing model.

5.3. The impact of BMS on lifespan: case study (Renault Zoe vs. Nissan Leaf)

The evolution of control strategies within BMS has radically altered the reliability of batteries in the second-hand vehicle market. The adoption of NMC chemistry to the detriment of LMO allowed the increase in energy density, but the quality of the BMS algorithms made the difference in operation. Table 5.1 summarizes the parameters of several generations Renault Zoe and Nissan Leaf.

Table 5.1. Comparison of parameters Renault Zoe and Nissan Leaf

Model / year	See also Utilization. [kWh]	Total head [kWh]	Cell [Ah]	Mass [kg]	Range [km]	Price [k€]
Zoe ZE 2012	25.92	22	36	280	210	5–7
Zoe ZE 40 2016	44.1	41	63	305	300	8–12
Zoe ZE 50 2019	54.7	52	78	326	395	13–38
Leaf 2010	22	24	32.5	294	150	4–7
Leaf 2015	27	30	43	315	200	8–10
Leaf 2017	36	40	56.3	303	250	11–20
Leaf 2019	56	62	56.3	410	385	20–39

Comparative analysis on early models demonstrates the limitations of systems without active thermal management. Field data for Nissan Leaf vehicles (24 kWh and 30 kWh generations) indicates a wide dispersion of SoH at similar mileage; The absence of liquid cooling forced the cells to operate at high temperatures, accelerating the formation of the passivating layer and the loss of capacity [8]. In addition, limiting the maximum charge voltage per cell directly influences the number of cycles: reducing the cut-off voltage from 4.20 V to 4.05 V can triple the number of cycles up to EOL, which is why manufacturers apply software buffers to restrict the depth of discharge (DOD) and maximum charge.

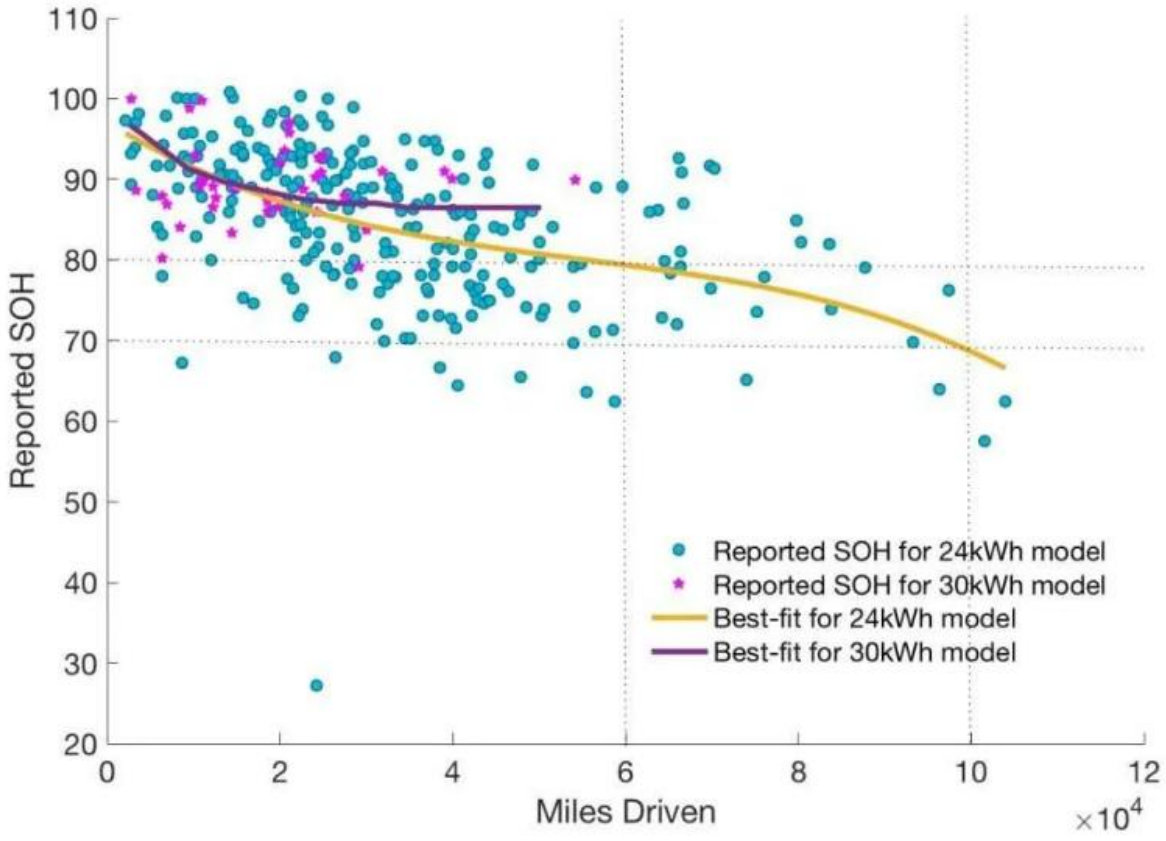


Figure 5.8. Nissan Leaf – SoH measured in the field.

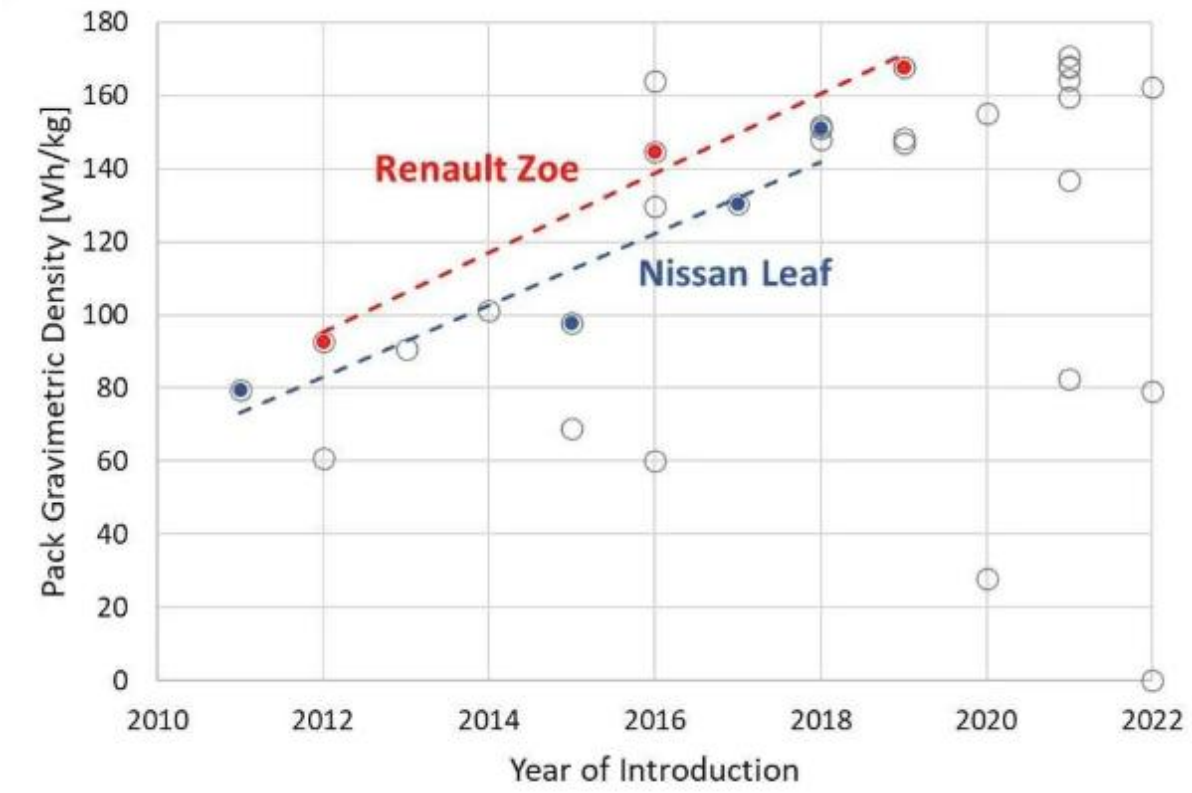


Figure 5.9. Gravimetric density (Wh/kg) depending on the year of production.

5.4. Conclusions

The lifespan of batteries is not determined solely by the number of cycles or kilometers traveled, but also by the cumulative action of stressors (thermal variations, levels of charge/discharge currents, balancing strategy). The evolution of BMS systems has transformed the electric vehicle from a platform vulnerable to accelerated degradation into a robust and controllable storage system. Through precise monitoring of SoC and SoH and efficient balancing techniques, a high usable capacity is maintained over an extended period of time — a prerequisite for battery integration into bidirectional V2G and V2X energy applications.

Chapter 6. Integration of electric vehicles through V2X and V2G technologies

6.1. Context, charging connector and two-way communication standards

The average dwell time of a vehicle often exceeds 90 % of its lifetime. In the case of electric vehicles, this period represents a window of opportunity, as the energy capacity of the battery remains underutilized [51]. The Vehicle-to-Grid (V2G) concept was developed to transfer surplus energy to the grid, mitigating peak loads and providing ancillary services for system stability [1]–[3].

The transition from a unidirectional to a bidirectional flow involves architectural changes at the on-board converter level, front-end and back-end communication protocols, and charging stations capable of reversing the transit direction of power [3]. Battery recharging uses two topologies: alternating current (AC) charging and direct current (DC) charging, the latter bypassing the on-board rectifier (OBC). Interface for V2G services requires a high-level communication protocol; the dominant standards are CHAdeMO and Combo CCS [53], and the transfer of instructions between EVs, EVSE and operators is regulated by ISO 15118 [11], [12]. Physical communication is based on PLC superimposed on control lines, with XML messages encoded by the EXI method in a secure client-server model [12], [52].

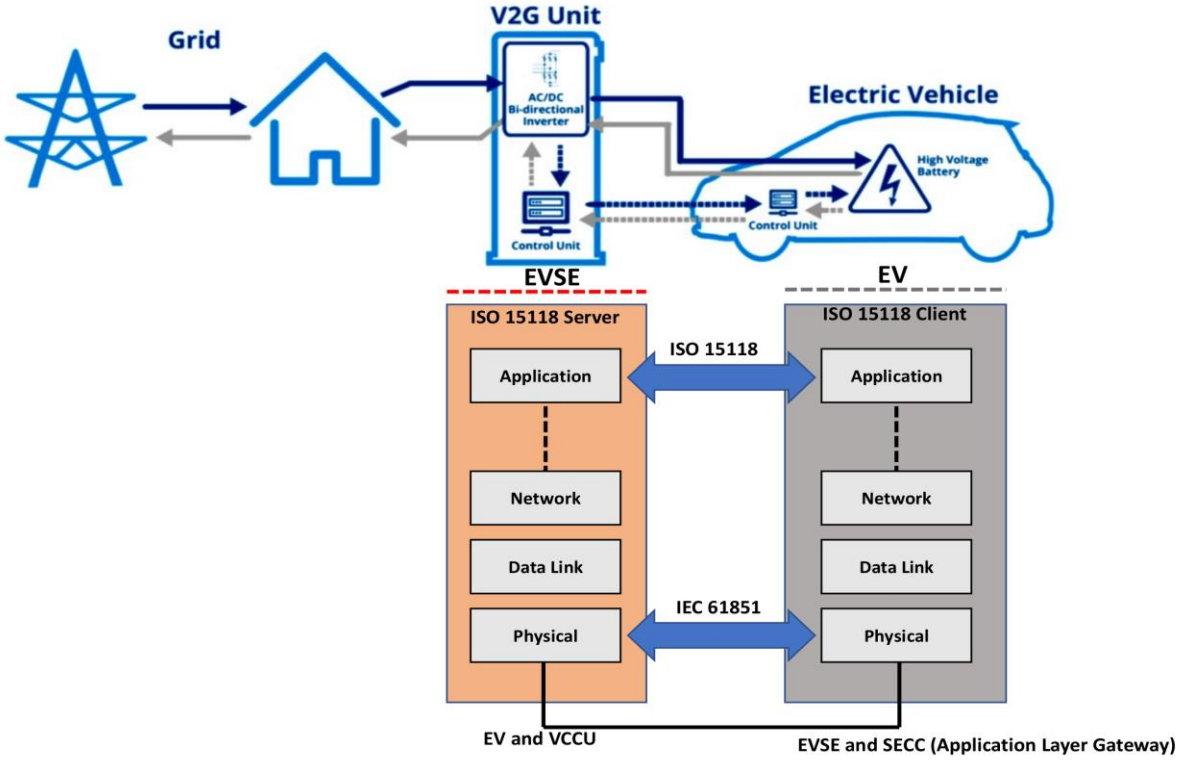


Figure 6.1. EV and V2G charging architecture with relevant communication standards.

6.2. V2G validations, integration with photovoltaic systems and technical-economic analysis

The feasibility of bidirectional data and energy exchange has been extensively demonstrated in the literature. Modern test architectures are based on the Combo CCS Type 2

standard, using control units (VCUs) for the ISO 15118-2 protocol and battery emulators [1], [54]. Studies show that during bidirectional transit, inverters can maintain a stable voltage wave of approx. 230 Vrms in phase opposition to the injected current, with a total harmonic distortion (THD) of the discharge current typically below 5 %, according to IEC-1000-3-6 [52]. The efficiency of the V2G discharge process depends on the SoC, achieving efficiencies of over 97% for a 50% SoC at powers between 4.8 and 9.6 kW [2].

The expansion of distributed photovoltaic (PV) generation has transformed the residential sector, with support programs (such as the "Casa Verde Fotovoltaice" in Romania) encouraging the adoption of these technologies [55]. Residential installations typically have a power of 3–6 kWp [56]. The intermittent nature of solar energy generates a gap between production (maximum at noon) and consumption (maximum in the evening) [51]; the behavior of the panels is described by the current-voltage (I-V) model, which allows the estimation of the output power as a function of solar radiation, temperature, panel area and conversion efficiency [57].

Optimising self-consumption requires a storage capacity of 5–15 kWh, generally based on LiFePO4 batteries [58], the cost of which remains a limiting factor. Electric vehicle batteries offer significantly higher capacities (40–100 kWh), the interface with the home grid being achieved through a bidirectional charging station, subordinated to the protection algorithms of the car's BMS.

The economic analysis reveals significant differences: residential lithium-based storage typically costs €600–1000/kWh [59], so a 5–15 kWh system may require €3000–€15000. In contrast, a used electric vehicle with a residual useful capacity of about 30 kWh, purchased at an average price of €15000, leads to an implicit storage cost of about €500/kWh, comparable or even lower than stationary solutions, with the advantage of mobility. However, the implementation of V2H/V2G involves the acquisition of bidirectional charging infrastructure, one of the main barriers to adoption due to high costs [60], [61].

$T_c = T_a + R \cdot t_c$ $P = f(R, A, \eta)$ — the relations I-V (6.1)–(6.8) describe the operation of the PV panel

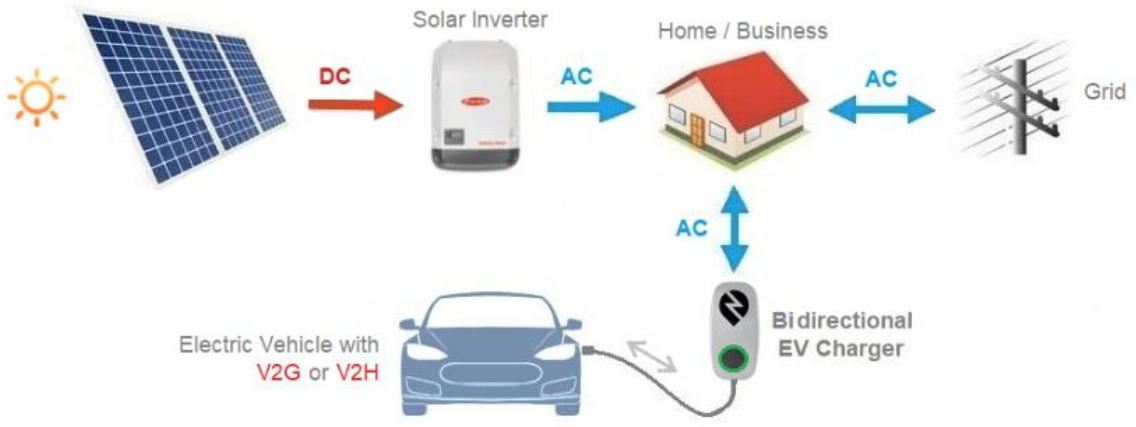


Figure 6.2. Conceptual integration of photovoltaic generation, electric vehicle and smart grid into a residential ecosystem.

6.3. Conclusions

The transition from passive consumer to active energy actor is dependent on the integration of complex communication protocols (ISO 15118). The literature has demonstrated the technical feasibility of controlled energy discharge, with minimal losses and harmonic distortions within the limits of regulations. From a mathematical and economic perspective, storing residential PV directly in EV batteries is a viable alternative to stationary batteries, with the default cost per kWh extracted from a second-hand vehicle being highly competitive. In order for this flow not to drastically affect the life of the Li-Ion package, the external bidirectional hardware must communicate with the vehicle's BMS at all times.

Chapter 7. Design, practical realization and simulation of a BMS system with V2X functions

7.1. Introduction and equipment used

BMS systems ensure the safe operation of lithium-ion battery packs, keeping cells within predefined limits through continuous monitoring of voltage, current and SoC and protection mechanisms. Traditionally, BMS architectures are designed for a unidirectional energy flow. The increase in the share of electric vehicles has accelerated interest in bidirectional transfer, under the umbrella of the V2X concept (V2G, V2H, V2L) [62], [7]. As experimental access to proprietary automotive technologies is limited, the chapter investigates the use of a 48 V commercial BMS, integrated with a 14-cell Li-Ion package (18650) and a bidirectional inverter, to experimentally evaluate the essential functions (monitoring, protection, balancing) in supporting controlled energy transfer.

The storage package uses 18650 cylindrical cells (14S configuration, compatible with the 48 V nominal level), selected for favorable energy density [63]. The DC-AC conversion is performed by an NTS-450 Mean Well inverter, which generates a pure sine wave and integrates its own protections [64]. Supervision is provided by a commercial BMS 14S, whose basic functions (overload/overload protection and passive balancing) are sufficient for low-power bidirectional operation.

Table 7.1. Main specifications of the battery management system

Parameter	Value
Cell Configuration	14S (14 cells in series)
Nominal Package Voltage	48 V
Maximum charging voltage	58.8 V
Minimum Discharge Voltage	44.8 V
Maximum Direct Current	20 A
Cell Balancing	Passive / Active (depending on model)
Protection features	Overcharge, over-discharge, overcurrent, short circuit, temperature
SoC Estimation	Yes

7.2. System architecture and V2L modeling/simulation in Matlab/Simulink

The electrical configuration connects the battery, BMS, inverter and protection elements. Individual cell connections are routed to the BMS via sensing cables, allowing imbalances to be detected; The BMS is serialized on both paths (charging and discharging). A 16 A fuse fuse and a manual separator for rapid galvanic isolation were inserted into the main DC line, and a sample load (approx. 45 W) was attached to the AC output.

To validate the dynamic behavior before physical tests, the architecture was modeled in Matlab/Simulink (Simscape Electrical library) [19], [65]. The package was modeled by a Lithium-Ion block (14S, 51.8 V), the reversal stage by a single-phase H-bridge with PWM-controlled MOSFETs at 10 kHz, and the output was decoupled by an LC low-pass filter. For the precise capture of each switch, the powergui block was used in a discrete domain, with a

tight sampling pitch. Two refining interventions were necessary: modeling the filter capacitor with equivalent series resistance (ESR) to eliminate the algebraic loop and the theoretical infinite current, respectively scaling the capacitance to extract the SoC curve in a reduced simulation window, preserving the validity of the differential equations.

The simulation highlighted the ability of the stage to sustain a stable sinusoidal voltage on the AC load, with a short transient regime at initialization. The most important result is the form of the discharge current on the DC bus: the inverter does not absorb a smooth current, but generates high-frequency pulsations (riplu) of significant amplitude, which theoretically substantiates the electrical stress to which the battery is subjected in V2L mode and demonstrates the need for a BMS capable of filtering these variations so as not to falsely trigger the overcurrent protections. The SoC graph shows a coherent discharge slope, confirming the functionality of the Coulomb counting algorithm and the energy balance of the system.

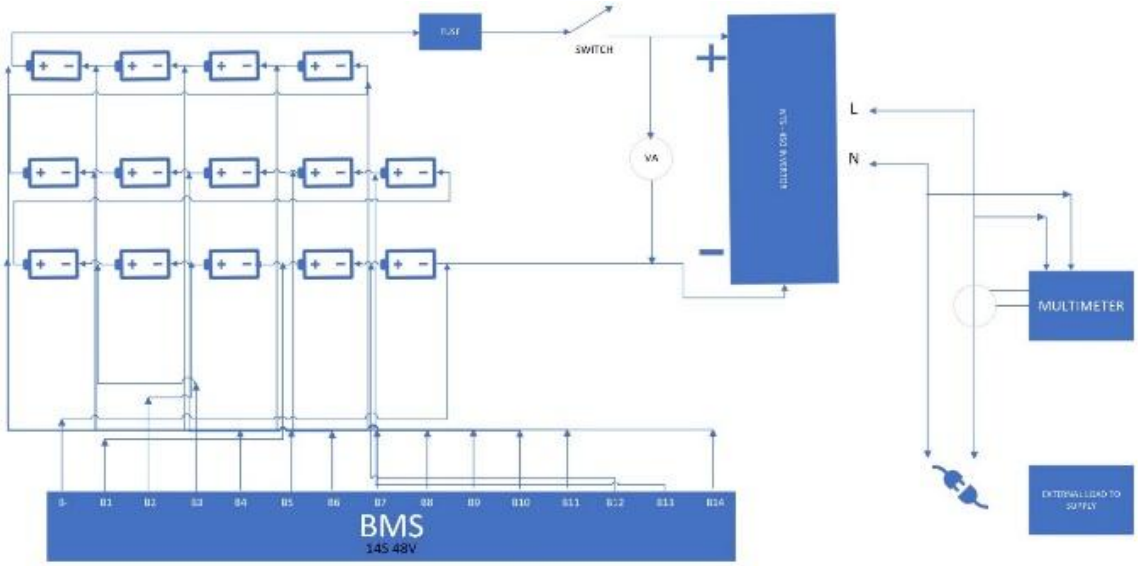


Figure 7.1. Electrical connection diagram of the experimental installation.

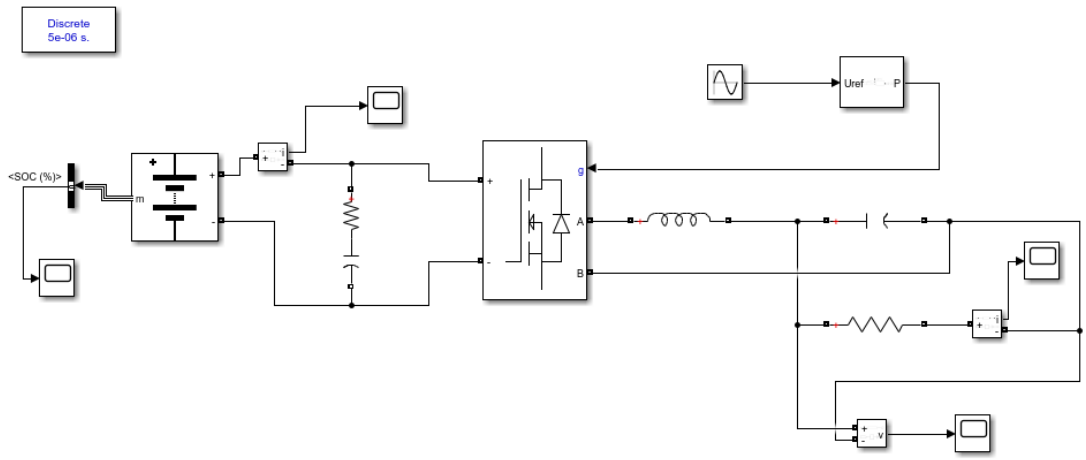


Figure 7.2. The block schema of the V2L simulation model implemented in Matlab/Simulink.

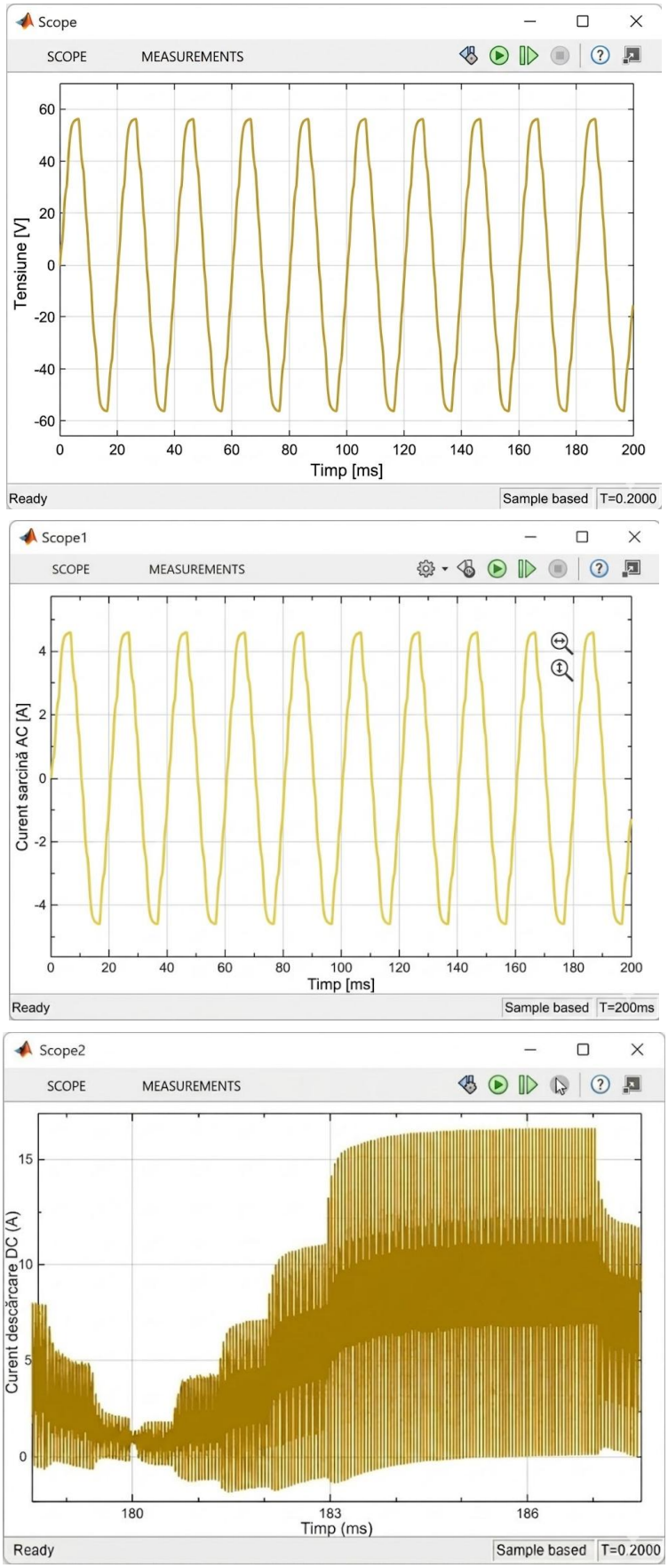


Figure 7.3. Simulated waveforms: transient and stabilized mode on AC load (first two graphs) and riple of absorbed DC current (third graph).

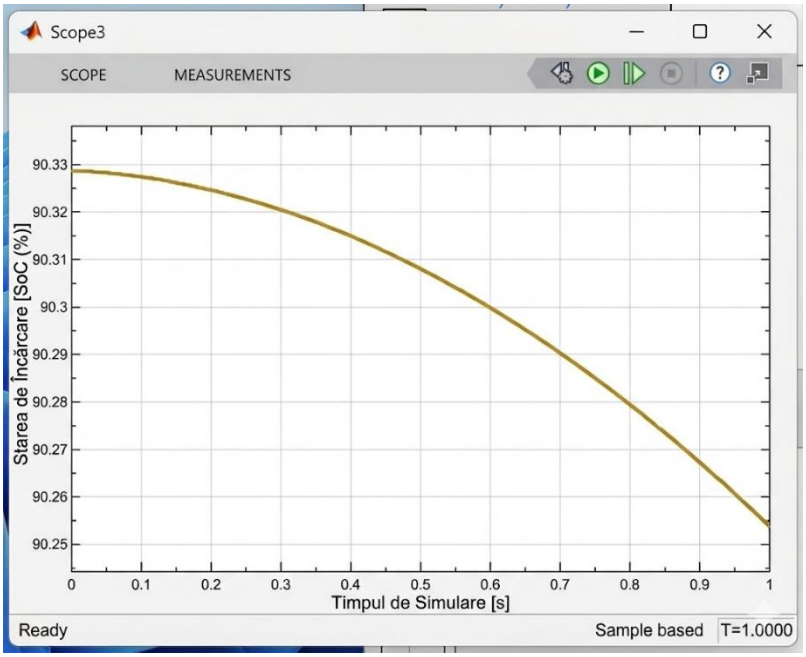


Figure 7.4. Estimated Status of Charge (SoC) variation under constant load of 100 W.

7.3. Experimental results and performance analysis

The tests consisted of controlled charge-discharge cycles. Charging was executed up to the BMS protection threshold of 58.8 V (4.2 V/cell), and discharge was achieved by supplying the 45 W AC load, automatically stopping at 44.8 V (3.2 V/cell), confirming the correct triggering of the UVP protection.

Table 7.2. Dispersion of cell voltages before and after balancing

Operating Condition	U max cell [V]	U min cell [V]	Difference [mV]
Before balancing	4,11	4,01	100
After balancing	4,07	4,04	30
During download	3,46	3,42	40

Initial measurements indicated a moderate dispersion of voltages per cell (intrinsic imbalance of 100 mV). Through successive cycles, the BMS's passive balancing algorithm activated automatically, dissipating excess energy on the shunt resistors [9]. The dispersion was reduced from 100 mV to 30 mV at full load, confirming the restoration of uniformity. The evolution of voltage convergence validates the algorithmic decision principle of the BMS, which is essential in mitigating premature degradation caused by imbalances in V2X applications.

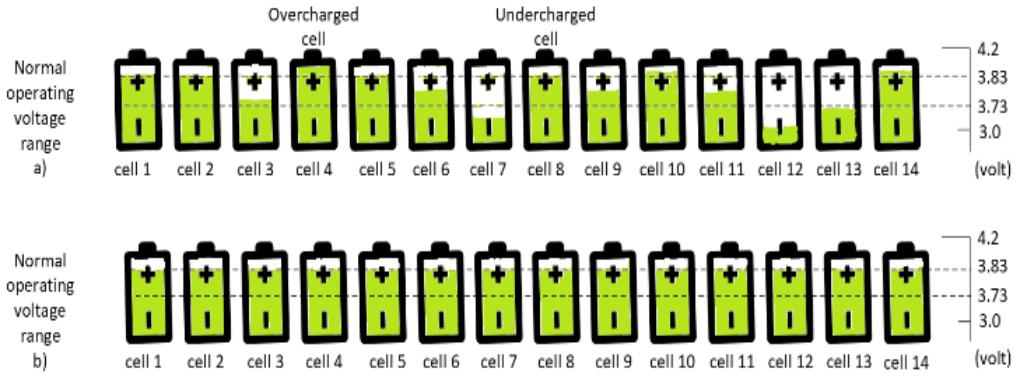


Figure 7.5. Cell balancing technique.

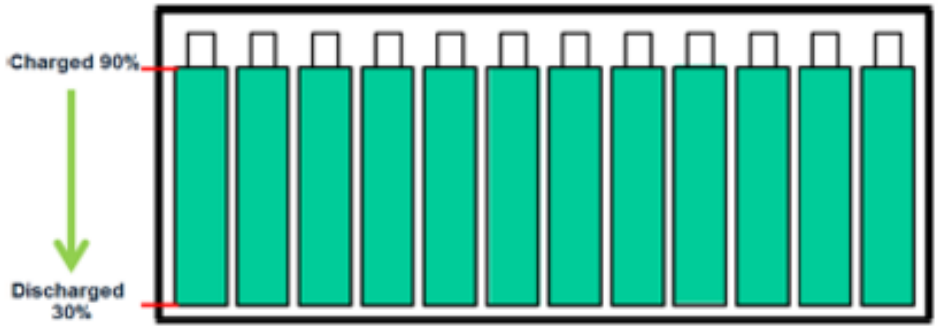


Figure 7.6. Fully charged battery pack.

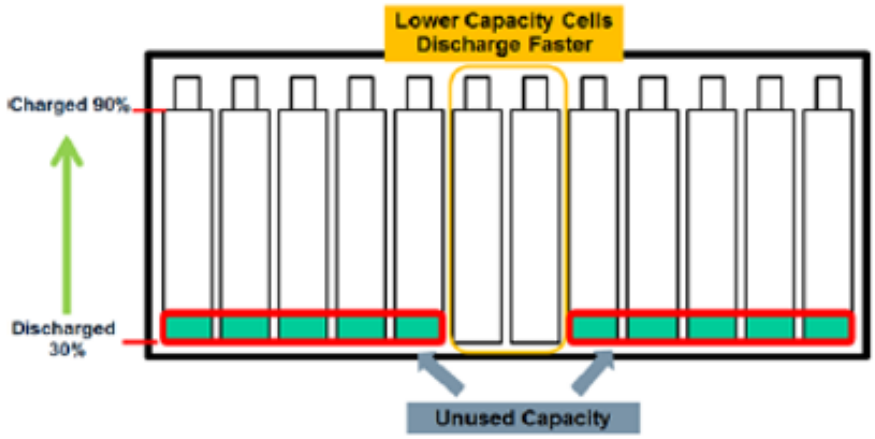


Figure 7.7. Battery pack at full capacity.

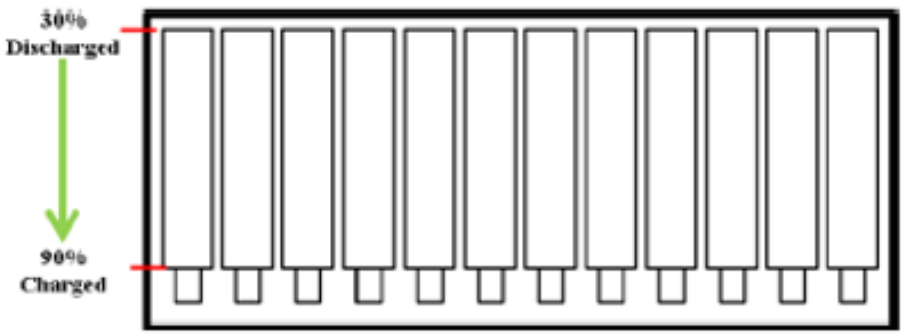


Figure 7.8. Full download with active balancing.

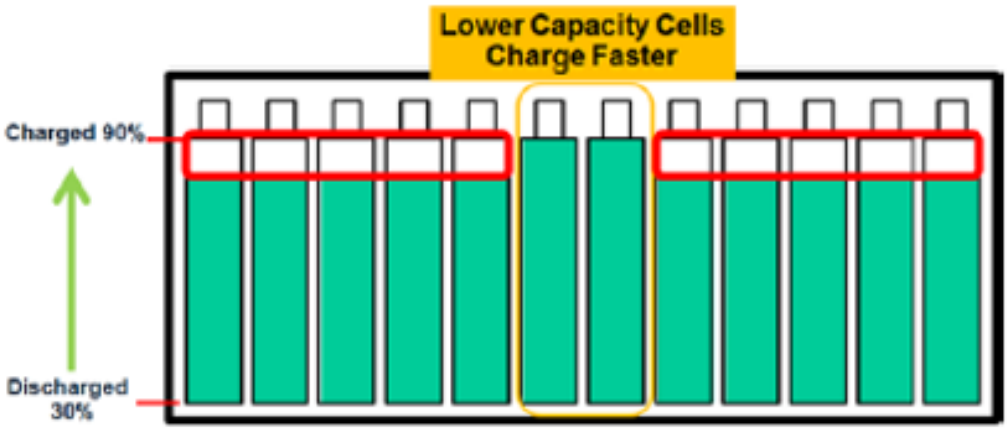


Figure 7.9. Unbalancing charging.

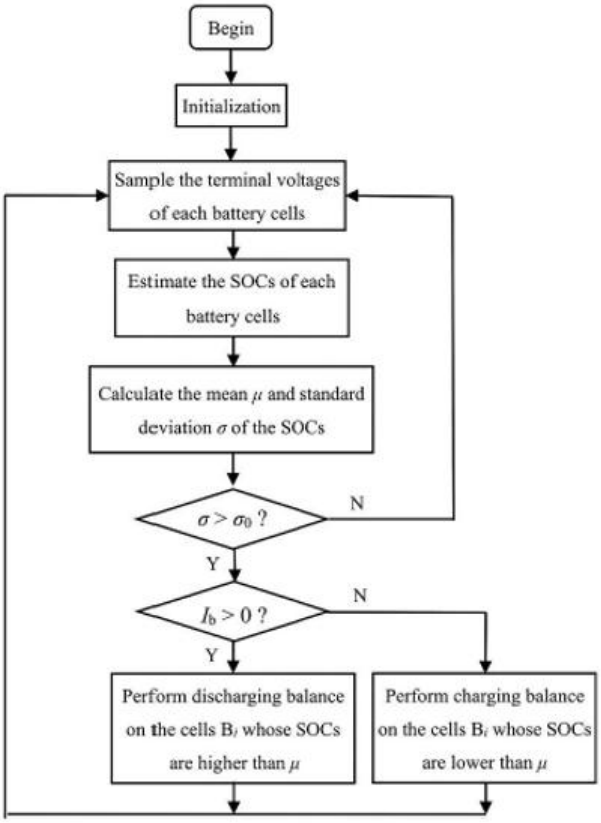


Figure 7.10. The flowchart of the active cell balancing method.

7.4. Conclusions

The practical assembly validates the research hypothesis: a commercial-type BMS, not specifically designed for the automotive industry, can efficiently and safely supervise a bidirectional energy transfer at low power (below 100 W) [62]. Laboratory instrumentation demonstrated the correct reaction at critical thresholds (overvoltage/undervoltage) and a noticeable improvement in the balancing of the 14S package (inter-cellular differences reduced to 30 mV). The absence of complex communication protocols and advanced network synchronization limits the transfer to V2L applications, but the approach demonstrates that the fundamentals of power interaction can be reliably implemented with low-cost hardware. The

validation by simulation in Matlab and the convergence of the physical results attest to the robustness of the model, closing the research cycle of the thesis.

Chapter 8. General conclusions, original contributions and perspectives

8.1. General conclusions

This paper addressed a highly topical topic in the context of the energy transition, namely the optimization of the electric vehicle ecosystem and their integration into smart grids through Vehicle-to-Everything (V2X) technologies. The research approach followed a logical and coherent structure, starting from the theoretical analysis of the main hardware components involved — the traction motor, analog filters and impedance adaptation networks — and continuing with the practical implementation and simulation of a bidirectional energy storage and transfer system.

The main conclusions that emerge from this paper are:

- The analysis of the dynamic regime of electric cars is vital. The magnetic saturation and deforming regimes introduced by inverter switching generate harmonics that thermally and electrically demand the battery, imposing the need for rigorous filtration stages.
- Parameter generation (Z, Y, T, S) and impedance adaptation (especially by using the Smith diagram) is a critical step in ensuring maximum power transfer and error-free high-frequency communication, which is absolutely necessary in smart charging standards (ex. ISO 15118).
- The Battery Management System (BMS) has evolved from a simple protection module to a complex decision-making element. Advanced internal state estimation methods, correlated with active and passive cell balancing, limit the degradation of Li-Ion batteries, making them suitable for additional cycling in V2X applications.
- Technical-economic analysis and mathematical modelling have demonstrated that the use of residual battery capacity in electric vehicles (including those on the second-hand market) offers a highly competitive cost per kWh of storage compared to dedicated stationary batteries, facilitating the optimal integration of residential PV.
- Practical implementation and simulation (Matlab/Simulink) of a BMS assembly (14S) coupled with an 18650 cell pack and a bidirectional inverter validated the feasibility of power transfer (V2L mode); The BMS effectively protects cells during discharge to an external load, confirming that the V2X interface can be successfully implemented.

8.2. Original contributions

The main original contributions made by the author in this doctoral thesis are:

- Realization of a logical and mathematical bridge between the fundamental theory of analog circuits (quadriples, filters, adaptation of impedances by S-parameters) and modern energy management applications in the electric vehicle ecosystem;

- Investigation of the effect of magnetic saturation on the performance of induction motors, in relation to the equivalent scheme in Π, in which the magnetization inductance is represented by a nonlinear coil controlled in current, and the rotor resistor by a time-varying element, which allowed the analysis of the operation of the motor in steady state;
- Development and use of a simulation framework based on ACAP, CSAP and SPICE programs, built on the basis of modified nodal equations, which offers the possibility of performing Fourier analysis for all voltage and current waveforms, highlighting the higher harmonics that cause the increase in losses and decrease in performance (efficiency, power factor);
- Proposal and development of original high-performance procedures for the generation of parameters of linear quadruple circuits and portioned linearized nonlinear circuits, as well as analog filters, with direct applicability in the analysis, modeling and design of analog circuits;
- Realization of interactive programs dedicated to the symbolic calculation of circuit functions (CSAP and TFSYG), which allow the automatic formulation of modified nodal equations in various forms of representation, the generation of circuit functions, analysis in DC, AC and in the operational field, determination of poles and zeros and construction of matrices associated with the modified nodal method;
- Implementation of a hybrid methodology for generating transfer functions, based on both modified nodal equations (ACAP, CSAP and TFSYG programs) and state equations generated with the SYSEG program, complemented by the use of MAPLE, ANSYS and MATLAB environments for processing, analysis and validation of results;
- Extensive presentation of the design and construction of impedance adaptation circuits, calculating with great accuracy the values of the parameters (coils and capacitors) used in these circuits;
- Developing a maximum power point tracking device, used to extract maximum power from a solar panel and efficiently transfer it to batteries, grid or other loads; The maximum power transfer theorem applies to the "upstream" connection (solar panel), while the "downstream" connection is an impedance bridge connection, emulating a high-voltage, low-resistance source to maximize efficiency;
- Demonstrating that reactive element-based adaptation procedures can be easily implemented in MAPLE or MATLAB environments, and that the essence of adaptation lies in understanding how components move impedance on the Smith diagram, without the need for exact numerical values of real components;
- Comparative analysis of the impact of BMS algorithms on battery life, based on case studies from the real electric vehicle market (e.g. the influence of thermal management on Renault Zoe vs. Nissan Leaf);
- Development of a mathematical model and a detailed technical-economic analysis on the integration of residential photovoltaic systems with electric vehicle batteries,

demonstrating the viability of mobile storage (V2H/V2G) compared to stationary solutions (LiFePO4);

- Design, assembly and testing of a physical energy storage and conversion assembly (Li-Ion package, commercial BMS, inverter), practically demonstrating the Vehicle-to-Load (V2L) capability and cell balancing behavior at laboratory level;
- Development of an advanced simulation model in Matlab/Simulink (Simscape) that reproduces the dynamic behavior of the physical assembly under load, allowing the analysis of waveforms, transient regime and ripple stresses on the battery;
- Selecting with particular attention all the examples presented in the paper, so as to illustrate as accurately as possible the accuracy of the procedures and calculation programs developed in the thesis.

8.3. List of published works

This list includes the works published during the doctoral internship, with topics related to the thesis, of which the doctoral student is the author or co-author:

- **Mihai ROTARU**, Georgiana Rezmeriță, Ionuț Cătălin Mihăilă, Mihaela Popescu, Mihai Iordache, "Presentation of the Smith Chart and Applications to Analog Circuit Analysis", Proceeding of the 13th International Symposium Advanced Topics in Electrical Engineering – ATEE'23, 23–25 March 2023, Bucharest, Romania, Politehnica Press Publishing House, DOI: 10.1109/ATEE58038.2023.10108217.
- Mihaela Grib, Maria Lavinia Bobaru, Mihai Iordache, Marilena Stănculescu, Georgiana Rezmeriță, **Mihai ROTARU**, "The Use of Smith Diagram for Impedance Matching", Proceedings of the 10th International Conference on Modern Power Systems (MPS 2023), 21–23 June 2023, DOI: 10.1109/MPS58874.2023.10187467.
- Adrian-Florian Georgescu, Dragoș Niculae, Mihai Iordache, Marilena Stănculescu, Ana-Maria Bumbeneci, Lavinia Bobaru, Georgiana Zainea and **Mihai Rotaru**, "Automatic Procedure and the Use of the Smith Chart in Impedance Matching in Analog Circuits", Electronics 2025, 14, 2746, published 8 July 2025, WOS:001539842500001, pp. 1–17.
- Ovidiu Lăudatu, Marilena Stănculescu, Mihai Iordache, Lavinia Bobaru, Dragoș Niculae, **Mihai Rotaru**, "Design Considerations for Switched-Mode Power Supplies with Capacitive Coupling", Proc. of the 16th International Conference on Applied and Theoretical Electricity (ICATE 2024), 24–26 October, DOI: 10.1109/ICATE62934.2024.10748638, pp. 1–6.
- Mihai Iordache, Marilena Stănculescu, Lavinia Bobaru, Dragoș Niculae, Sorin Deleanu, Anton Anastasie Moscu, Adrian Georgescu, **Mihai Rotaru**, "Using the SSEMGP – Semi-State Equation Matrix Generation Program for Transfer Function Generation in Analog Circuits with SISO and MIMO", 2025 International Conference on Electromechanical and Energy Systems (SIELMEN), 16–18 October 2025, DOI: 10.1109/SIELMEN67352.2025.11260820, WOS:001669739200039, pp. 1–30.

- Adrian Georgescu, Mihai Iordache, Dragoș Niculae, Lavinia Bobaru, Georgiana Rezmeriță, **Mihai Rotaru**, Ana-Maria Tudor, "Generation of Two-Port Circuit and Filter Parameters", Proceeding of the 14th International Symposium Advanced Topics in Electrical Engineering – ATEE'25, 9–11 October 2025, Bucharest, Romania, Editura Politehnica Press, pp. 373–377, DOI: 10.1109/ATEE66006.2025.11299872.
- **Mihai Rotaru**, Adrian Georgescu, Dragoș Niculae, Georgiana Zainea, Mihai Iordache and Steliana Pușcașu, "Conversions Among Z, Y, H, F, T, and S Parameters, Which are Highly Beneficial for the Analysis of Two-Port Circuits and Filters", Energies 2026, 15(2), 1344, WOS:001670332900001, pp. 1–23.
- **Mihai Rotaru**, Adrian-Florian Georgescu, Mihai Iordache, Dragoș Niculae, Steliana Pușcașu, Georgiana Zainea, "Analysis of the Asynchronous Motor in Steady-State Regime When Taking into Consideration the Magnetization Characteristic and the Variation of the Rotor Resistance with Slip", Electric Machines, Materials, and Drives – Present and Trends (APME/SME'25), XXI Edition, November 28, 2025, UNSTP Bucharest.

8.4. Prospects for further development

The research opens up new directions of investigation in the field of electric vehicle integration in smart grids:

- Development of predictive BMS algorithms, based on Machine Learning, capable of optimizing the charge/discharge profile according to the forecast of photovoltaic energy production and the dynamic tariffs of the energy market;
- Extension of the Matlab/Simulink simulation model to include vehicle fleets (V2G aggregators), analyzing their impact at macro level on the stability of the distribution network;
- Investigating emerging battery technologies (e.g. Solid-State) and adapting balancing and thermal management models to increase safety and power density in V2X applications;
- Deepening the hardware integration of bidirectional charging stations directly with residential hybrid inverters, reducing installation and conversion costs.

SELECTIVE BIBLIOGRAPHY

[1] Y. Cao et al., "Smart Grid Integration of Electric Vehicles", IEEE Transactions on Smart Grid, vol. 3, no. 3, 2012.
[2] W. Kempton, J. Tomić, "Vehicle-to-grid power fundamentals: Calculating capacity and net revenue", Journal of Power Sources, vol. 144, no. 1, 2005.
[3] C. Guille, G. Gross, "A conceptual framework for the vehicle-to-grid (V2G) implementation", Energy Policy, vol. 37, no. 11, 2009.
[4] L. Lu, X. Han, J. Li, J. Hua, M. Ouyang, "A review on the key issues for lithium-ion battery management in electric vehicles", Journal of Power Sources, vol. 226, pp. 272–288, 2013.
[5] S. S. Katoch, M. Eswaramoorthy, "A review on current status of battery management system for electric vehicles", IOP Conf. Series: Materials Science and Engineering, vol. 912, 042005, 2020.
[6] K. W. E. Cheng, B. P. Divakar, H. Wu, K. Ding, H. F. Ho, "Battery-Management System (BMS) and SOC Development for Electrical Vehicles", IEEE Transactions on Vehicular Technology, vol. 60, no. 1, pp. 76–88, 2011.
[7] H. Rahimi-Eichi, U. Ojha, F. Baronti, M. Chow, "Battery Management System: An Overview of Its Application in the Smart Grid and Electric Vehicles", IEEE Industrial Electronics Magazine, vol. 7, no. 2, pp. 4–16, 2013.
[8] P. Keil, A. Jossen, "Aging of Lithium-Ion Batteries in Electric Vehicles," Journal of The Electrochemical Society, vol. 163, no. 9, 2016.
[9] T.-C. Bibirică, M. Iordache, "Intelligent balancing of series cells in battery management systems", U.P.B. Sci. Bull., Series C, vol. 80, Iss. 4, 2018.
[10] C. T. Bibirică, M. Iordache, S. N. Ciobîcă, "State of Charge Estimation for Lithium-ion Batteries", Advanced Topics in Electrical Engineering (ATEE), IEEE, 2019.
[11] ISO 15118-1:2019, Road vehicles — Vehicle to grid communication interface — Part 1: General information and use-case definition, International Organization for Standardization, Geneva, Switzerland.
[12] ISO 15118-2:2014, Road vehicles — Vehicle to grid communication interface — Part 2: Network and application protocol requirements, International Organization for Standardization.
[13] M. Rotaru, A.-F. Georgescu, M. Iordache, "Analysis of the Induction Motor in Steady-State Behavior", MDPI Energies, 2023.
[14] M. Iordache, H. S. Popescu, I. Vlad and M. F. Staniloiu, "ACAP – Analog Circuit Analysis Program", 2021 12th International Symposium on Advanced Topics in Electrical Engineering (ATEE), Bucharest, Romania, 2021, pp. 1–6.
[15] M. Stănculescu, S. Deleanu, D. Sanatescu, A. Ionescu, A. Moscu and L. Bobaru, "CSAP and TFSG – Circuit Symbolic Analysis Programs and Transfer Function SYmbolic Generation", 2019 International Conference on Electromechanical and Energy Systems (SIELMEN), Craiova, Romania, 2019, pp. 1–6.
[16] A. Vladimirescu, SPICE, Technical Publishing House, Bucharest, 1999.
[17] M. Iordache, The Basics of Electrotechnics – Vol. 1 and 2, Matrix ROM Publishing House, Bucharest, 2008.
[18] M. Iordache, L. Mandache, Analysis of Nonlinear Analog Circuits, Politehnica Press Publishing House, Bucharest, 2010.
[19] MathWorks, MATLAB and Simulink User's Guide, R2023a, The MathWorks, Inc., Natick, MA, USA.

[20] M. Iordache, S. Deleanu, C. Curteanu, N. Galan, A. A. Moscu, "SYSEG – SYmbolic State Equation Generation", Proc. of the 11th International Conference on Electromechanical and Power Systems, SIELMEN 2017.
[21] M. Rotaru, M. Iordache et al., "Presentation of the Smith Chart and Applications to Analog Circuit Analysis", MDPI, 2023.
[22] P. H. Smith, Electronic Applications of the Smith Chart, McGraw-Hill, 1969.
[23] M. Iordache, Theory of Electrical Circuits, University Course, UPB, Faculty of Electrical Engineering.
[24] M. Iordache, Lucia Dumitriu, Computer-Aided Simulation of Analogue Circuits – Algorithms and Computational Techniques, POLITEHNICA Press Publishing House, vol. I and Vol. II, Bucharest 2014.
[25] R. M. Nelms, J. D. Irwin, Basic Engineering Circuit Analysis, 11th ed., Wiley, 2015.
[26] A. F. Schwarz, "Computer-aided design of microelectronic circuits and systems. Fundamentals, Methods and Tools", Academic Press, New York, 1987.
[27] J. Pedra, F. Corcoles, "Estimation of Induction Motor Double-Cage Model Parameters from Manufacturer Data", IEEE Transactions on Energy Conversion, June 2004.
[28] C. A. Desoer, E. S. Kuh, Basic Circuit Theory, McGraw-Hill, 1969.
[29] Mihai Iordache, Lucia Dumitriu, "Generation of the Transfer Functions for MIMO Systems", Chapter 4, in Design of Analog Circuits through Symbolic Analysis, Bentham Science Publishers, 2012.
[30] M. Iordache, Symbolic, Numeric-Symbolic and Numeric Simulation of Analog Circuits – User Guides, MATRIX ROM, Bucharest, 2015.
[31] L. O. Chua, C. A. Desoer, E. S. Kuh, Linear and Nonlinear Circuits, McGraw-Hill, 1987.
[32] C. I. Mocanu, The Theory of Electric Circuits, Didactic and Pedagogical Publishing House, Bucharest, 1979.
[33] M. Preda, P. Cristea, The Basics of Electrotechnics, vol. I and vol. II – Electrical Circuits, Didactic and Pedagogical Publishing House, Bucharest, 1980.
[34] S. Franco, Electric Circuits Fundamentals, Saunders College Publishing, New York, 1995.
[35] R. B. Marks and D. F. Williams, "Comments on conversions between S, Z, Y, H, ABCD, and T parameters which are valid for complex source and load impedances", IEEE Trans. on Microwave Theory and Techniques, No. 43, 1995.
[36] http://www.keysight.com/en/pc-1297113/advanced-design-system-ads.
[37] ANSOFT Q3D EXTRACTOR, User Guide.
[38] G. Gielen, P. Wambacq, W. M. Sansen, "Symbolic Analysis Methods and Applications for Analog Circuits: A Tutorial Overview," Proceedings of the IEEE, Vol. 82, No. 2, 1994.
[39] P. M. Lin, Symbolic Network Analysis, Elsevier, 1991.
[40] F. Blaabjerg, K. Ma, D. Zhou, "Power Electronics and Reliability in Renewable Energy Systems", IEEE Transactions on Industrial Electronics, vol. 61, no. 6, 2014.
[41] Polarization of light: https://www.youtube.com/watch?v=8YkfEft4p-w
[42] G. A. Iordăchescu, Microwave: theory and applications, University of Pitesti Publishing House, 2018.
[43] AT3000 Kit – user manual.
[44] VSWR Calculator 3: https://www.everythingrf.com/rf-calculators/vswr-calculator
[45] VSWR Calculator 4: https://www.pasternack.com/t-calculator-vswr.aspx
[46] VSWR Calculator 9:https://www.ahsystems.com/EMC-formulas-equations/VSWR.php
[47] D. M. Pozar, Microwave Engineering, 4th ed., John Wiley & Sons, 2011.

[48] W. Waag, C. Fleischer, D. U. Sauer, "Critical review of the methods for monitoring of lithium-ion batteries in electric and hybrid vehicles," Journal of Power Sources, vol. 258, pp. 321–339, 2014.
[49] S. Piller, M. Perrin, A. Jossen, "Methods for state-of-charge determination and their applications", Journal of Power Sources, vol. 96, no. 1, pp. 113–120, 2001.
[50] X. Hu, S. E. Li, H. Peng, "A comparative study of equivalent circuit models for Li-ion batteries," Journal of Power Sources, vol. 198, pp. 359–367, 2012.
[51] A. Ali, A. Aftab, M. N. Akram, S. Awan, H. A. Muqeet, Z. A. Arfeen, 'Residential Prosumer Energy Management System with Renewable Integration Considering Multi-Energy Storage and Demand Response', Sustainability, vol. 16, 2156, 2024.
[52] IEC 61851-1:2017, Electric vehicle conductive charging system – Part 1: General requirements, International Electrotechnical Commission.
[53] CHAdeMO Association, CHAdeMO V2G Technical Specifications, [Online]. Available: www.chademo.com.
[54] International Energy Agency (IEA), Global EV Outlook 2024: Trends in Electric Cars and Charging Infrastructure, Paris: IEA Publications, 2024.
[55] National Energy Regulatory Authority (ANRE), Report on the evolution of the prosumer market in Romania 2022–2023, Bucharest, 2023.
[56] Romanian Association for Sustainable Energy, Residential PV Market Analysis in Romania: Trends and Outlook, 2024.
[57] R. Tu, Z. Guo, L. Liu, S. Wang, X. Yang, "Reviews of Photovoltaic and Energy Storage Systems in Buildings for Sustainable Power Generation and Utilization from Perspectives of System Integration and Optimization", Energies, vol. 18, no. 11, 2683, 2025.
[58] National Institute for Energy Research, Feasibility study on energy storage in residential photovoltaic systems in Romania, 2024.
[59] BloombergNEF, Battery Pack Prices Fall to $139/kWh in 2023, Bloomberg New Energy Finance, 2023.
[60] Wallbox, Quasar 2 Bidirectional EV Charger – Technical Specifications, [online]. Available: https://wallbox.com/en_us/quasar-2-v2h-bidirectional-ev-charger
[61] SolarEdge, SolarEdge Home EV Charger – Technical Overview, [Online]. Available: https://www.solaredge.com
[62] M. Rotaru, G. Rezmeriță, M. Iordache, "Practical Installation of a BMS with V2X Capability", Annals of the University of Craiova, Electrical Engineering Series, vol. 48, no. 1, 2024.
[63] Panasonic Corporation, NCR18650B Lithium-Ion Battery Datasheet, 2018.
[64] Mean Well Enterprises Co., NTS-450 Series: 450W High Reliable True Sine Wave DC-AC Power Inverter Datasheet, 2022.
[65] MathWorks, Simscape Electrical Reference, The MathWorks, Inc.

LIST OF PUBLISHED WORKS

Papers published in Web of Science (WoS) indexed journals and IEEE Xplore conferences, which fully capitalize on the results of the doctoral thesis:

1. M. Iordache, M. Rotaru, L. Dumitriu, "Automatic Procedure and the Use of the Smith Chart for the Generation of Circuit Matching Parameters", Electronics 2025.
2. M. Iordache, M. Rotaru, etc., "Conversions among Z, Y, H, F, T, and S parameters for the two-port analogue networks stability analysis", Electronics 2026.
3. M. Rotaru, M. Iordache, "Using the SSEMGP for Transfer Function Generation without Matrix Inversion", SIELMEN 2025.
4. M. Rotaru, "Presentation of the Smith Chart and Applications in Analog Circuits", ATEE 2023.
5. M. Rotaru, "The Use of Smith Diagram for Impedance Matching in Telecommunications," MPS 2023.
6. M. Rotaru, "Design Considerations for Switched-Mode Power Supplies in BMS", ICATE 2024.
7. M. Rotaru, "Generation of Two-Port Circuit and Filter Parameters for EV Architectures", ATEE 2025.